

Optimizing Spray-Dried Liposomes for Pulmonary Delivery: Impact of Lipids Composition and of Drying Parameters using experimental design

Laure-Anne Bya^a, Tuan Nghia Dinh^a, Noémie Penoy^a, Pierre-Yves Sacré^b, Benedetta Bottero^c, Didier Cataldo^c, Erika Hendrickx^d, Louise Conrard^d, Brigitte Evrard^a, Géraldine Piel^a, Anna Lechanteur^{*a}

^aUniversity of Liege, Laboratory of Pharmaceutical Technology and Biopharmacy, Center for Interdisciplinary Research on Medicines (CIRM), Avenue Hippocrate 15, 4000 Liege, Belgium

^bUniversity of Liege, CIRM, Research Support Unit in Chemometrics, Department of Pharmacy, Avenue Hippocrate 15, 4000 Liege, Belgium

^cUniversity of Liege, Laboratory of Tumor and Development Biology, GIGA-Cancer, Avenue Hippocrate 15, 4000 Liege, Belgium

^dCenter for Microscopy and Molecular Imaging (CMMI), Université Libre de Bruxelles (ULB), B-6041 Gosselies, Belgium

*Corresponding author

Mail: anna.lechanteur@uliege.be

Phone: +3243663847

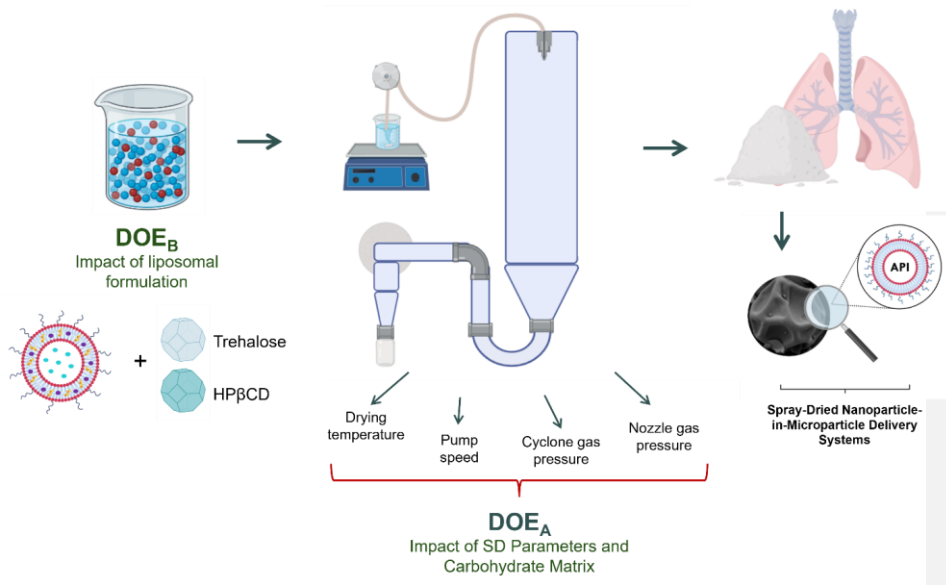
ABSTRACT

Liposomes are promising carriers for pulmonary drug delivery due to their biocompatibility and controlled-release properties. However, their stability in aqueous suspension is limited, leading to aggregation and reduced therapeutic efficiency. Converting liposomal dispersions into dry powders for inhalation (DPIs) is a potential strategy to overcome these limitations. Spray-drying (SD) is particularly attractive for this purpose, offering precise control over particle properties along with speed, cost-efficiency, and scalability. Yet, the thermal and mechanical stresses involved in this process and their effects on liposomal integrity remain poorly understood, limiting its broader application.

In this study, we developed a systematic framework integrating Design of Experiments (DOE) with scale-up-oriented processing, combining supercritical fluid technology (PGSS) for liposome formation with subsequent spray-drying of high solid content suspensions. Two complementary DoE approaches were applied: DOE_A optimized drying parameters and carbohydrate type, testing trehalose and hydroxypropyl- β -cyclodextrin (HP β CD), while DOE_B assessed the effects of active pharmaceutical ingredients (APIs) hydrophobicity, lipid composition (1,2-Distearoyl-sn-glycero-3-phosphoethanolamine-N-[methoxy(polyethylene glycol)-2000 (DSPE-PEG₂₀₀₀) percentage), and carbohydrate-to-liposome ratio.

Optimized spray-dried powders exhibited preserved liposome structure (mean diameter <200 nm, narrow polydispersity index (Pdl), near-neutral zeta potential (ZP)), favorable aerodynamic properties (\sim 3 μ m, extra-fine particle fraction (eFPF) >20% and fine particle fraction (FPF) >60%), low residual moisture (<5%), and high drying yields (>75%). Mechanistic insights revealed that HP β CD significantly protects liposomes during atomization, while drug retention was governed by PEGylated lipid content, lipid-to-carbohydrate ratio, and API hydrophobicity. Co-encapsulation of clinically relevant drug combinations (formoterol/budesonide and ciclesonide/indacaterol) produced uniform powders with efficient aerosolization, highlighting the therapeutic potential of these formulations.

Collectively, these results establish a robust, scalable, and reproducible approach for designing liposomal DPIs, balancing formulation composition, excipient selection, and process parameters. This study demonstrates that strategic integration of scalable technologies can reconcile structural stability, aerodynamic performance, and manufacturability, paving the way for the industrial translation of liposomal dry powders for targeted pulmonary therapies, including asthma and chronic obstructive pulmonary disease (COPD).



KEYWORDS

Dry powder inhalers

Liposome

Spray-drying

Design of Experiments

ABBREVIATION

API, Active Pharmaceutical Ingredient; BUD, Budesonide; Chol, Cholesterol; CIC, Ciclesonide; COPD, Chronic Obstructive Pulmonary Disease; Dae, Aerodynamic Diameter; DepthD, Depth of dimples; DSC, Differential Scanning Calorimetry; DOE, Design of Experiment; DSPE-PEG₂₀₀₀, 1,2-Distearoyl-sn-glycero-3-phosphoethanolamine-N-[methoxy(polyethylene glycol)-2000]; DPI, Dry Powder Inhaler; ED, Emitted Dose; FDA, U.S. Food and Drug Administration; FD, Freeze-Drying; FPD, Fine Particle Dose; FPF, Fine Particle Fraction; eFPF, extra-Fine Particle Fraction; FOR, Formoterol; GSD, Geometric Standard Deviation; glass transition temperature (T_g); HPβCD, Hydroxypropyl-β-Cyclodextrin; HPLC, High Performance Liquid Chromatography; ICS, Inhaled Corticosteroid; ICH, International Council for Harmonisation of Technical Requirements for Pharmaceuticals for Human Use; ICS, Inhaled Corticosteroid, IND, Indacaterol Maleate; Inlet temperatures (T^{°in}); outlet temperature (T^{°out}); LABA, Long-Acting Beta-2 Agonists, L/C ratio, Lipid-to-carbohydrate ratio; LOD, Limits of detection; LOQ, Limits of quantification; MMAD, Mass Median Aerodynamic Diameter; NGI, Next Generation Impactor; PE, Péclet Number; pMDI, Pressurized Metered-Dose Inhaler; Pdl, Polydispersity Index; PSD, Particle Size Distribution; PGSS, Particles from Gas-Saturated Solutions; RD, Recovery Dose; RH, Relative Humidity; RSD, Relative Standard Deviation; SABA, Short-Acting Beta-2 Agonist, SAL, Salbutamol; SD, Spray-Drying; SEM, Scanning Electron Microscopy; SGC, Supercritical CO₂ (scCO₂); SMI, Soft-Mist Inhaler; SPC, Soy Phosphatidylcholine; TGA, Thermogravimetric Analysis.

1. Introduction

1 Liposomes have emerged as highly promising carriers for pulmonary drug delivery, a potential
2 recently highlighted by the U.S. Food and Drug Administration (FDA) approval of Arikayce® in
3 2018, a liposomal amikacin suspension for inhalation (Bashyal et al., 2025; Pasero et al.,
4 2024). Their biocompatibility, capacity to encapsulate both hydrophilic and lipophilic drugs,
5 membrane-like structure, tunable size, and ability to enhance retention and enable controlled
6 release highlight their strong pharmacological potential (Senjab et al., 2024; Zhang et al.,
7 2025). Additionally, liposomes can penetrate the mucus layer and overcome mucociliary
8 clearance, addressing a major barrier to efficient pulmonary drug delivery and reinforcing their
9 promise as advanced respiratory drug carriers (Lin et al., 2025; Yan & Sha, 2023). When
10 combined with the intrinsic advantages of pulmonary administration, namely targeted lung
11 delivery, rapid onset, limited drug degradation, and minimal systemic side effects, liposomal
12 formulations offer significant opportunities for more effective inhaled therapies (Cipolla et al.,
13 2013).

14 Despite these beneficial attributes, aqueous liposomal suspensions are prone to aggregation
15 and fusion over time, which can reduce therapeutic efficacy (Xu et al., 2025). To address this
16 limitation, liposomes can be converted into dry formulations, with dry powder inhalers (DPIs)
17 offering a particularly promising approach in the field of inhalation therapy (Yu et al., 2021).
18 Furthermore, unlike conventional inhalation devices such as nebulizers, metered-dose inhalers
19 (pMDIs) and soft-mist inhalers (SMIs), DPIs bypass propellant gases and nebulization, thereby
20 reducing the risk of liposomal disruption during delivery while extending shelf-life (Rudokas et
21 al., 2016; Shahin & Chablani, 2023). Beyond improved stability, DPIs enable precise particle
22 engineering, allowing control over size, surface charge, moisture content, and morphology,
23 which critically influence dispersibility, stability, and deep lung deposition (Chaurasiya & Zhao,
24 2021; Negi et al., 2023; Scherließ et al., 2022; Spahn et al., 2022).

25
26 Liposomal dispersions can be converted into dry powders using well-established techniques
27 such as freeze-drying (FD) and spray-drying (SD) (Negi et al., 2023). Among these, SD is
28 particularly suited for DPIs production, allowing fine control over particle attributes. Indeed,
29 when carefully optimized, this approach yields powders with consistent aerodynamic
30 properties and enhanced pulmonary deposition (Alhaji et al., 2021; Lechanteur & Evrard,
31 2020), whereas FD typically produces an irregular, lyophilized cake with inadequate flowability
32 (Vishali et al., 2019). Furthermore, from an industrial perspective, SD is also considerably
33 faster, more cost-effective, and highly reproducible (Ziaee et al., 2019). Yet, while FD has been
34 extensively documented for liposomal drying across a wide range of applications (Furst et al.,
35 2016; Kaialy & Nokhodchi, 2013; Nugraheni et al., 2017), the use of SD for liposomal powder
36 formulation remains comparatively less investigated, largely due to the additional challenges
37 of preserving liposomal integrity under this atomizing process. These challenges arise from
38 the structural characteristics that make liposomes attractive carriers, most notably their flexible
39 bilayer and aqueous core, which simultaneously make them highly vulnerable to shear,
40 thermal, and dehydration stresses. Such stresses (high inlet temperatures and atomization
41 pressures) can compromise membrane integrity, leading to drug leakage, vesicle fusion, or
42 even collapse (Dattani et al., 2025; Safaeian Laein et al., 2024). In this context, a suitable
43 carbohydrate matrix is crucial to protect liposomes during drying and ensure efficient
44 aerosolization.
45

46
47 In the pulmonary context, early work by Goldbach et al. (Goldbach et al., 1993) showed that
48 multilamellar soybean phosphatidylcholine (SPC) liposomes spray-dried with 10% lactose
49 retained vesicle size and phospholipid stability upon reconstitution, establishing SD as a viable
50 approach for producing stable pulmonary liposomal powders. However, subsequent studies
51 revealed that SD can induce vesicle shrinkage or transitions from uni- to bi-lamellar structures,

52 underscoring the need for protective excipients (Wessman et al., 2010). In this regard,
53 cyclodextrins, specifically HP β CD, have been shown to stabilize PEGylated liposomal
54 membranes during SD, preventing bilayer disruption and drug leakage (Van Den Hoven et al.,
55 2012). Trehalose similarly enhances product yield while preserving liposome size and drug
56 encapsulation, and, with or without L-leucine, enables the production of stable, re-dispersible
57 lipid-based powders (Dattani et al., 2025; Khan et al., 2024). Furthermore, Meenach et al.
58 demonstrated that PEGylation facilitates the SD of particles, preserving the bilamellar
59 phospholipid structure post-drying while ensuring favorable aerodynamic performance suitable
60 for pulmonary delivery (Meenach et al., 2013).

61
62 Taken together, these studies provide important proof that liposomes can be successfully
63 processed by SD when appropriately formulated and protected. However, most investigations
64 have primarily focused on end-point characterization, offering limited insight into the underlying
65 formulation and process relationships required to derive transferable design principles. As a
66 result, the successful development of liposomal DPIs demands not only confirmation of
67 liposomal integrity, but also a systematic understanding of how formulation and process
68 parameters collectively govern vesicle preservation while enabling inhalation-relevant powder
69 properties. This gap has been explicitly highlighted in the literature, as
70 Ingvarsson et al. (Ingvarsson et al., 2011) noted that liposome integrity following SD is
71 frequently assumed rather than systematically investigated, despite being a critical quality
72 attribute for inhalable liposomal products.

73
74 To address this, the present study systematically investigates how SD parameters and
75 formulation strategies influence liposome integrity and DPI quality. A Quality by Design
76 approach based on Design of Experiments (DOE) was applied, integrating formulation
77 development with scale-up-oriented processing. Liposomes were prepared using supercritical
78 fluid technology (PGSS), a solvent-free, one-step process that overcomes key limitations of
79 conventional solvent-based methods, thereby supporting industry-relevant manufacturing
80 (Delma et al., 2023; Penoy et al., 2022), and subsequently dried via SD. An initial DOE
81 evaluated the influence of drying parameters at three distinct levels and compared two
82 carbohydrate matrices, trehalose and HP β CD, for their stabilizing effects on liposomes.
83 Despite the lack of current approval for pulmonary administration, the restricted excipient
84 landscape for inhalation motivates the investigation of well-characterized carbohydrates to
85 broaden the formulation design space and inform regulatory assessment. Subsequently, a
86 second DOE examined the impact of liposomes variables, including active pharmaceutical
87 ingredients (APIs) hydrophobicity, lipid composition (varying the percentage of PEGylated
88 lipid), and carbohydrate-to-liposome ratio. By incorporating APIs with markedly different
89 physicochemical properties, the robustness and transferability of the formulation-process
90 relationships were specifically assessed. Following the identification of optimal drying
91 conditions, structural stability of the liposomes was evaluated across the industrial processes
92 (PGSS and SD), while *in vitro* aerodynamic performance was assessed using a Next
93 Generation Impactor (NGI) to determine their suitability for pulmonary delivery.

94 Overall, this study aimed to develop optimized DPIs containing PEGylated liposomes capable
95 of delivering multiple APIs. Formulations were designed to preserve liposome integrity while
96 achieving physicochemical properties favorable for inhalation and increased deep lung
97 deposition. This strategy enables the co-encapsulation of agents such as inhaled
98 corticosteroids and β 2-agonists, which are recommended for asthma and COPD therapy. To
99 demonstrate the robustness of this approach, clinically used APIs, namely salbutamol (SAL),
100 budesonide (BUD), formoterol (FOR), ciclesonide (CIC), and indacaterol (IND), were
101 deliberately selected to span a broad range of physicochemical properties, particularly in terms
102 of hydrophilicity/lipophilicity and molecular structure, thereby enabling assessment of the

103 transferability of the formulation–process relationships across diverse APIs. The inclusion of
104 underexplored combinations such as CIC with the ultra-long-acting β 2-agonist IND further
105 underscores the translational potential of these liposomal DPIs for future combination
106 therapies.

107

108 2. Materials and methods

109

2.1. Materials

110 Micronized ciclesonide (CIC, 98.9%) was kindly supplied by NewChem spa (Milan, Italy), and
111 indacaterol maleate (IND, 99.5%) was obtained from LEAP Chem CO (Wan Chai, Hong Kong).
112 Micronized budesonide (BUD, 100.2%) was supplied from Minaken (Dunkerque, France),
113 while salbutamol base (SAL, 99.7%) was purchased from Cambrex (Milan, Italy). Formoterol
114 fumarate dihydrate (FOR, 100.4%) was supplied sourced CHEMA Industriale chimica
115 (Saronno, Italy). All APIs were employed as model compounds in this study.

116 SPC was purchased from Avanti Polar Lipids, Inc. (Alabaster, AL, USA), cholesterol (CHOL)
117 from Sigma Aldrich (Brussels, Belgium) and 1,2-distearoyl-sn-glycero-3-
118 phosphoethanolamine-N-[methoxy(polyethyleneglycol)-2000] (ammonium salt) (DSPE-
119 PEG₂₀₀₀) from Xiamen Sinopeg Biotech (Xiamen, China).

120 Tested carbohydrates, including hydroxypropyl- β -cyclodextrin (HP β CD) and Vialose™
121 trehalose dihydrate, were kindly provided by Roquette (Lestrem, France) and Asland
122 (Schaffhausen, Switzerland), respectively. Saccharose (biochemistry grade) was purchased
123 from Sigma-Aldrich (Darmstadt, Germany).

124 High-performance liquid chromatography (HPLC)-grade methanol and absolute ethanol were
125 sourced from J.T. Baker (Deventer, The Netherlands) and ThermoFisher Scientific (Geel,
126 Belgium), correspondingly. Ammonium acetate, 25% ammonia solution, 4-(2-
127 hydroxyethyl)piperazine-1-ethanesulfonic acid (HEPES, $\geq 99.5\%$), and sodium chloride were
128 all obtained from Sigma-Aldrich (St. Louis, MO, USA, and Brussels, Belgium). Analytical-grade
129 potassium phosphate was sourced from Merck (Darmstadt, Germany), while sodium heptane
130 sulfonate was acquired from VWR Chemicals (Leuven, Belgium). Ultrapure water (resistivity
131 of 18.2 M Ω ·cm) was produced using a Milli-Q purification system (Millipore), followed by
132 filtration through 0.22 μ m Millipak® 40 disposable filter units (Millipore Corporation, MA, USA).
133 Liquid CO₂ with a purity of 99.7% was purchased from Air Liquide (Zaventem, Belgium).

134 Size 3 hydroxypropyl methylcellulose capsules suitable for inhalation were supplied by
135 Capsugel® from Lonza Colmar, France) and used in combination with the Breezhaler® from
136 Novartis Pharma BV (Basel, Switzerland), a low-resistance inhalation device characterized by
137 a resistance of 0.0177 (kPa)^{0.5}·(min·L⁻¹), as reported in previous studies (Abadelah et al.,
138 2018; Dal Negro, 2015).

139

140 2.2. API quantification

141 The quantification of CIC, IND, BUD, FOR, and SAL was carried out using an Agilent 1100
142 Series HPLC system (Santa Clara, USA) equipped with a UV detector. The analytical methods
143 were successfully validated using the accuracy profile approach, with Enoval® software version
144 3.0 (Arlenda, Liège, Belgium).

145 2.2.1. Ciclesonide and Indacaterol maleate

146 For the analysis of CIC and IND, separation was achieved using an XBridge BEH C18
147 analytical column (3 × 50 mm, 3.5 μ m), preceded by a VanGuard Cartridge pre-column.
148 Detection was performed at 243 nm. The mobile phase consisted of an ammonium acetate
149 buffer (pH 10) and methanol, using the following gradient program: 0-1 min: 80/20 (v/v); 1-10

150 min: linear gradient to 5/95; 10-13 min: isocratic 5/95; 13.5-20 min: return to 80/20. The flow
151 rate was 0.7 mL/min. Column and sampler temperatures were maintained at 30 °C and 10 °C,
152 respectively. Sample preparation involved dilution in methanol (at least 10-fold) to disrupt the
153 liposomal structures and enable accurate quantification of APIs. For this method validation, a
154 10% risk level (α) and acceptance limits of 10% were defined over the concentration ranges
155 of 1 to 100 µg/mL for CIC and 2 to 100 µg/mL for IND. Accuracy profiles were constructed
156 using weighted linear regression ($1/X$) for both APIs. The lower limits of detection (LOD) and
157 quantification (LOQ) were 0.4600 µg/mL and 3.205 µg/mL for CIC, and 0.6153 µg/mL and
158 2.031 µg/mL for IND, respectively.

159 2.2.2. Budesonide and Formoterol fumarate dihydrate

160 BUD and FOR quantification employed the same column and detection wavelength (243 nm)
161 as those employed for the quantification of CIC and IND. The mobile phase also consisted of
162 ammonium acetate buffer (pH 10) and methanol, with a different gradient: 0-1 min: 55/45 (v/v);
163 1-2 min: linear gradient to 35/65; 2-7 min: isocratic 35/65; 8-20 min: return to 55/45. The flow
164 rate, column, and sampler temperatures were identical to the CIC and IND quantification
165 method. Sample preparation involved dilution in methanol (at least 10-fold) to disrupt the
166 liposomal structures and enable accurate quantification of APIs. For method validation, a 10%
167 risk level (α) and acceptance limits were set at $\pm 10\%$ over the concentration ranges of 1 to 100
168 µg/mL for BUD and 0.1 to 10 µg/mL for FOR. Accuracy profiles for BUD and FOR were
169 constructed using their respective selected calibration models: weighted quadratic regression
170 ($1/x^2$) for BUD and weighted linear regression ($1/x^2$) for FOR. For BUD, LOD and LOQ were
171 determined to be 0.2899 µg/mL and 4.395 µg/mL, respectively. For FOR, the LOD was
172 measured at 0.1161 µg/mL, with a corresponding LOQ of 0.9282 µg/mL (Lechanteur et al.,
173 2022).

174 2.2.3. Salbutamol

175 For SAL quantification, separation was performed using a LiChrospher® 100 RP8 column
176 (Hibar® RT 150 × 4.6 mm, 5 µm) under isocratic conditions. The mobile phase comprised of
177 phosphate buffer (pH 3.65) containing sodium heptane sulfonate (as an ion-pairing agent) and
178 acetonitrile (78:22 v/v). The flow rate was 1 mL/min, with the column maintained at 30 °C.
179 Samples (20 µL) were injected at room temperature. Detection was performed at 220 nm.
180 Sample preparation involved a 2-fold dilution in 2.5% Triton X-100 solution, followed by a 5-
181 fold dilution in the mobile phase, to disrupt the liposomal structures and enable accurate
182 quantification of APIs. For the validation of this method, a risk level (α) was set at 5% with
183 acceptance limits at 10%, over the concentration of 0.5 to 20 µg/mL for SAL (Penoy et al.,
184 2022). LOD and LOQ were both determined and found to be equal to 0.039 and 0.13 µg/ml,
185 respectively.

186

187 2.3. Quality by design methodology

188 The first design of experiment (**DOE_A**) is a D-optimal design investigating the main effects, first-
189 order interactions and quadratic effects of the experimental factors. The design incorporated
190 one categorical factor with two levels: carbohydrate type (trehalose vs HPβCD) and four
191 continuous factors: atomization inlet temperature (60-120 °C), pump feed rate (25-150 rpm),
192 nozzle gas pressure (1-4 bar), and cyclone gas pressure (0.05-0.3 bar). The selection of the
193 experimental factors and their corresponding ranges was based on prior scientific knowledge,
194 preliminary experimental investigations, and practical constraints associated with the SD
195 equipment. Overall, the investigated ranges were chosen to remain within physically

196 meaningful and experimentally feasible limits, while being sufficiently broad to capture relevant
197 effects and interactions among the SD parameters. Experimental work was structured with
198 random blocks of two experiments each plus three central point replicates totaling 24
199 experiments. Responses included the SD yield, particle size, and residual moisture content,
200 as well as liposome size and polydispersity index (Pdl) to monitor liposome integrity. All
201 responses were log-transformed before fitting the model. The initial suspensions contained 5%
202 solid content with a 1:99 lipid-to-carbohydrate ratio and empty liposomes with a
203 SPC/CHOL/DSPE-PEG₂₀₀₀ (65/30/5, molar ratio) composition.

204 Non-significant effects for each response were removed leading to the common mixed effect
205 model for all responses of the following form:

$$206 \quad Y = \beta_0 + \beta_1 E + \beta_2 IT + \beta_3 F + \beta_4 NGP + \beta_5 CGP + \beta_6 E * IT + \beta_7 E * F + \beta_8 E * CGP + \beta_9 IT * F \\ 207 \quad + \beta_{10} IT * NGP + \beta_{11} IT * CGP + \beta_{12} F * NGP + \beta_{13} NGP * NGP + \gamma_j + \varepsilon$$

208 where Y is the modelled response β_i is the estimate of the fixed effect of the factor i , E is the
209 carbohydrate type, IT is the inlet temperature, F is the flowrate, NGP is the nozzle gas
210 pressure, CGP is the cyclone gas pressure, γ_j is the random estimate of the j^{th} block and ε is
211 the error term.

212 The second design of experiment (**DOE_B**) employed a split-plot A-optimal design to investigate
213 the main factors, first-order interactions and quadratic effects of the investigated factors. The
214 split-plot structure was required for practical reasons: the categorical factor API nature (BUD
215 and SAL for hydrophobic and hydrophilic models) and the continuous factor DSPE-PEG₂₀₀₀
216 content (2.5-10%) were selected as hard to change factors. The third factor investigated is the
217 liposome-to-carbohydrate (L/C) ratios (1:99-10:90). These variables were selected based on
218 prior knowledge that DSPE-PEG₂₀₀₀ content plays a key role in liposome stability through steric
219 stabilization and membrane protection (Allen & Cullis, 2013), and that the physicochemical
220 nature of the API significantly impacts drug retention in liposomal suspension (Eloy et al.,
221 2014), while also enabling evaluation of formulation feasibility under the selected SD
222 conditions. The evaluated responses included liposome size and Pdl to monitor liposome
223 integrity, with particular emphasis on the impact of the tested parameters on the API release
224 after SD. Particle size and residual moisture content were monitored but not modelled during
225 DOE_B. The solid content was held constant at 5% as well, while applying the optimal drying
226 parameters and carbohydrate type established in DOE_A.

227 The log transformed responses were modelled with the following mixed-effect model:

$$228 \quad Y = \beta_0 + \beta_1 API + \beta_2 LPEG + \beta_3 LC + \beta_4 API * LPEG + \beta_5 API * LC + \beta_6 LPEG * LC + \beta_7 LPEG \\ 229 \quad * LPEG + \beta_8 LC * LC + \gamma_j + \varepsilon$$

230 where Y is the modelled response β_i is the estimate of the fixed effect of the factor i , API is the
231 API nature factor, $LPEG$ is the DSPE-PEG₂₀₀₀ content, LC is the liposome-to-carbohydrate (L/C)
232 ratio, γ_j is the random estimate of the j^{th} whole plot and ε is the error term.

233 Both DOEs were constructed and analyzed using JMP Pro 18 software.

234 2.3.1. PGSS-based preparation of liposomal formulations

235 Liposomes composed of SPC, CHOL, and DSPE-PEG₂₀₀₀ in varying molar ratios were
236 produced using the Particles from Gas-Saturated Solutions (PGSS) technique, employing
237 supercritical carbon dioxide (scCO₂) as a dispersing agent. The process was carried out under
238 optimized conditions (30min contact with scCO₂, 500rpm agitation rate at 80 °C) previously
239 established by Penoy *et al.* (Penoy et al., 2021, 2022), using PGSS equipment (Separex,
240 France), which was also described in detail in their work.

241 The phospholipid dispersion and APIs were pre-dispersed in HEPES buffer (10 mM, pH 7.4) at
242 65 °C, followed by stirring at 1200 rpm on a hot plate stirrer for 15 minutes. The resulting
243 dispersion was then introduced into the PGSS system. In **DOE_A**, a pressure of 156 bar was
244 applied to produce 5 mM empty liposomes, while 240 bar was used in **DOE_B** for 45 mM loaded
245 ones.

246 Liposome dispersions collected after the PGSS process were purified by dialysis using
247 Spectra/Por[®] cellulose dialysis membranes with a molecular weight cutoff of 20 kDa and a
248 diameter of 10 mm (VWR Chemicals). Dialysis was performed at 4 °C under stirring at 200 rpm
249 for 3 hours, using 20 mL of HEPES buffer per 1 mL of liposome dispersion. The dialysis medium
250 was replaced every hour. Liposomes purified from unencapsulated BUD and SAL were used
251 in **DOE_B** while liposomes purified from free FOR, BUD, CIC and IND were spray-dried in
252 following experiments. This purification also enabled the determination of encapsulation
253 efficiency (EE) after PGSS production. EE (%) was determined as the percentage of the total
254 drug that remained encapsulated within the liposomes after purification, calculated from the
255 difference between the total drug content before purification and the amount of free drug
256 detected after dialysis.

257 2.3.2. Spray-drying of liposomal formulations

258 In both DOEs, powders were produced using a Procept 4 M8-Trix Formatrix spray-dryer,
259 equipped with a bi-fluid nozzle. The nozzle diameter was fixed at 0.4 mm. For each batch, 20
260 mL of solution, in which the components (liposomes and carbohydrate) were dissolved and
261 brought up to volume with Milli-Q water, was used for SD. The process yield for each
262 formulation was calculated using the equation provided in Eq. (1).

$$263 \text{Drying process yield (\%)} = \frac{\text{Amount of powder collected after atomization (g)}}{\text{Total amount of powder implemented in the atomized liquid (g)}} \cdot 100 \quad (1)$$

264 Drying conditions were set according to the outcomes of **DOE_A** and are detailed below.

265

266 2.4. Assessment of the glass transition temperature of carbohydrates

267 Differential Scanning Calorimetry (DSC) measurements were carried out using a Mettler-
268 Toledo instrument (Schwerzenbach, Switzerland) to evaluate the glass transition temperatures
269 (T_g) of the investigated carbohydrates. Samples were analyzed in sealed aluminum pans
270 under a nitrogen atmosphere (20 mL/min). The temperature was increased from 25 to 300 °C
271 at a constant heating rate of 5 °C/min.

272 2.5. Characterization of liposomes

273 2.5.1. Particle size, size distribution and zeta potential of liposomes

274 Liposomes were characterized in terms of Z-Average size (nm), polydispersity index (Pdl), and
275 zeta potential (ZP) (mV) after production by PGSS and following SD, which required a
276 rehydration step, using Dynamic Light Scattering (DLS). Measurements were performed at
277 25 °C and a fixed detection angle of 90° with a Malvern Zetasizer[®] Nano ZS (Malvern
278 Instruments, UK). Samples produced by the supercritical process and liposomes rehydrated
279 from dry powders in Milli-Q water were diluted in 10 mM HEPES buffer (pH 7.4) to reach an
280 attenuation value of approximately 7, ensuring an optimal particle concentration for reliable
281 measurements. To evaluate potential size changes after drying, a size ratio (S_f/S_i) was
282 calculated between liposomes rehydrated from the spray-dried powder (S_f) and freshly
283 prepared liposomes after PGSS production (S_i). For both measurements (S_i and S_f), freshly
284 prepared and reconstituted liposomes were dispersed in HEPES buffer (pH 7.4) and diluted to
285 achieve an attenuator value of 7 during DLS, ensuring optimal signal quality and reliable size
286 determination. According to Abassi *et al.*, a ratio of 1 indicates that the liposome size remained
287 unchanged after drying, reflecting acceptable colloidal stability throughout the drying process

288 (Abbassi et al., 2025). All measurements were performed in triplicate, and the mean values
289 were reported.

290 2.5.2. Structural characterization by microscopy analyses

291 For TEM analysis, nickel grids (300 mesh) coated with a continuous carbon film were glow-
292 discharged (Elmo, Cordouan Technologies) prior to use. A 20 μ L drop of sample was applied
293 onto the grid and incubated for 10 min at room temperature. The excess liquid was then blotted
294 with filter paper, and the grids were stained with 2% (w/v) uranyl acetate for 60 s. After staining,
295 the grids were gently washed by sequentially placing them on two drops of ultrapure water,
296 blotted, and air-dried before imaging. Samples were imaged using a Talos transmission
297 electron microscope (ThermoFisher Scientific) operating at 200 kV. Images were acquired
298 using Velox software (ThermoFisher Scientific) and a Ceta camera (ThermoFisher Scientific).

299 For cryo-TEM analysis, QUANTIFOIL[®] R1.2/1.3 200 mesh Cu grids were glow-discharged
300 using an ELMO glow discharge system (Cordouan Technologies) at a vacuum of 2.1×10^{-1}
301 mbar and a voltage of 1.7 V for 35s. Grids were then transferred to a Vitrobot Mark IV
302 (ThermoFisher Scientific) for a plunge-freezing procedure. A double application of the sample
303 was used: 3 μ L of the particle suspension was applied to the grid, followed by blotting (blot
304 force = 2, blot time = 4 s, wait time = 5 s). Immediately after the first blot, a second 3 μ L aliquot
305 of the same suspension was applied, followed by a final blot (blot force = 2, blot time = 4 s,
306 wait time = 0 s). Vitrified grids were transferred into a Talos transmission electron microscope
307 (ThermoFisher Scientific) and observed under cryogenic conditions at an accelerating voltage
308 of 200 kV. Images were acquired using EPU software (ThermoFisher Scientific) and a Falcon
309 III EC camera (ThermoFisher Scientific) at a magnification of 73,000x corresponding to a pixel
310 size of 0.14 nm/pixel for an electron dose of $21 \text{ e}^-/\text{Å}^2$.

311 2.6. Characterization of the dried powders

312 2.6.1. Particle size distribution (PSD)

313 Particle size distribution (PSD) of the powder samples was evaluated using laser diffraction
314 with a Malvern Mastersizer 3000[®] (Malvern Instruments, Worcestershire, UK), fitted with the
315 AeroS dry dispersion unit. A small amount of powder, approximately equivalent to a spatula
316 tip, was placed on the micro tray, suitable for low sample volumes, and dispersed using a
317 standard Venturi system. The analysis was conducted at a feed rate of 30% and an air pressure
318 of 4.0 bar, ensuring an obscuration range between 0.5% and 8.0%. Each measurement lasted
319 10 seconds. Data acquisition and PSD analysis were performed using the dedicated Malvern
320 Mastersizer software. All measurements were conducted in triplicate, and the mean values
321 were reported.

322 2.6.2. Residual moisture content

323 The residual moisture content of all spray-dried powders was determined shortly after
324 processing using Thermogravimetric Analysis (TGA; Perkin Elmer, Norwalk, CT). Samples
325 weighing between 5 and 15 mg were placed in platinum pans and heated from 25 °C to 150 °C
326 at a rate of 10 °C/min. This technique measures weight loss as the sample is exposed to
327 temperatures exceeding the evaporation point of water, allowing for accurate quantification of
328 residual water content based on the observed mass decrease. All measurements were
329 conducted in triplicate, and results are expressed as mean values.

330 2.6.3. Evaluation of dried powders homogeneity

331 The homogeneity of each powder batch was assessed by collecting five samples from different
332 locations within the powder bed, including both surface and depth. Samples were dissolved in
333 the appropriate mobile phase for API quantification by HPLC (Section 2.2). Blend uniformity
334 was expressed as the coefficient of variation (CV), calculated from the five samples. According
335 to the European Pharmacopoeia, powders with a CV $\leq 5\%$ for mean API recovery were
336 considered homogeneous.

337 2.6.4. Particle morphology

338 After gold metallization, the morphology of the powders obtained by SD was examined using
339 a TESCAN Clara scanning electron microscope equipped with a secondary electron detector.

340

341 2.7. Characterization of API leakage from liposomes post drying

342 After the collection of the lipid-based dry powder, an adequate amount of powder was
343 rehydrated in 3 mL of Milli-Q water. Once fully dissolved, 2 mL of the resulting liquid phase
344 were purified by dialysis using Spectra/Por[®] cellulose dialysis membranes (20 kDa molecular
345 weight cutoff, 10 mm diameter; VWR Chemicals). Dialysis was carried out at 4 °C under stirring
346 at 200 rpm for 3 hours, using 20 mL of dialysis medium per 1 mL of liposome dispersion. The
347 dialysis medium consisted of a saccharose solution adjusted to match the osmolarity of the
348 sample and was replaced every hour. This purification method was validated in triplicate and
349 enabled the quantification of API released from liposomes following the atomization process.
350 The amount of released API was determined by HPLC (Section 2.2), measuring the API
351 concentration after powder rehydration (total drug) and after dialysis (encapsulated drug), with
352 the released fraction calculated as indicated in Eq. 2 below:

353
$$\text{Drug release upon drying (\%)} = \frac{\text{Encapsulated drug (\mu g/mL)}}{\text{Total drug (\mu g/mL)}} \cdot 100 \quad (2)$$

354

355 2.8. In vitro lung deposition evaluation

356 In vitro aerosol performance was evaluated using a Next Generation Impactor (NGI; Apparatus
357 E, Copley, Nottingham, UK) following the guidelines outlined in the European Pharmacopoeia.
358 The NGI, comprising eight stages and a pre-separator, was connected to the inhalation device
359 via an appropriate mouthpiece adapter. Airflow was set at 100 L/min using a flow controller
360 (TPK; Copley, Nottingham, UK) and maintained for 2.4 seconds at each flow rate, or at 60
361 L/min for 4 s, respectively. The Breezhaler[®] (Novartis Pharma AG), a low-resistance DPI, was
362 employed for testing, with 20 capsules assessed per run to ensure that the resulting
363 concentrations fell within the calibration curve. Powder deposits collected from all stages of
364 the NGI, including the mouthpiece, capsules, and device, were rinsed with the appropriate
365 mobile phase and subjected to sonication to ensure complete solubilization of APIs, followed
366 by HPLC analysis.

367 The emitted dose (ED), representing the fraction of drug released from the inhaler, was
368 calculated as the sum of API masses from the induction port to the last NGI stage. The fine
369 particle dose (FPD) was defined as the portion of the dose consisting of particles with an
370 aerodynamic diameter below 5 μm. The fine particle fraction (FPF) was calculated relative to
371 the ED using the following equation (Eq.3):

372
$$FPF (\%) = \frac{\text{Mass of particles} < 5 \mu\text{m}}{\text{Emitted dose (ED)}} \cdot 100 \quad (3)$$

373 In addition, the extra-fine particle fraction (eFPF), defined as the fraction of particles with an
374 aerodynamic diameter below 2 μm, was calculated relative to the ED using the following
375 equation (Eq. 4):

376
$$eFPF (\%) = \frac{\text{Mass of particles} < 2 \mu\text{m}}{\text{Emitted dose (ED)}} \cdot 100 \quad (4)$$

377 The mass median aerodynamic diameter (MMAD) was determined from the cumulative mass
378 distribution of the aerosol, corresponding to the diameter at which 50% of the total aerosol
379 mass is contained. The geometric standard deviation (GSD) was calculated as the ratio of the
380 diameters at the 84th (D84) and 50th (D50) percentiles.

381

382 2.9. Statistical analysis

383 Data analysis was performed using GraphPad Prism software (version 8.4.3, La Jolla, CA,
384 USA). Results are presented as mean values accompanied by their standard deviations (SD).
385 Statistical differences among groups were assessed via analysis of variance (ANOVA),
386 followed by Tukey's post hoc multiple comparison test. Statistical significance was defined as
387 p-values less than 0.05 (*), 0.01 (**), or 0.001 (***)).

388

389

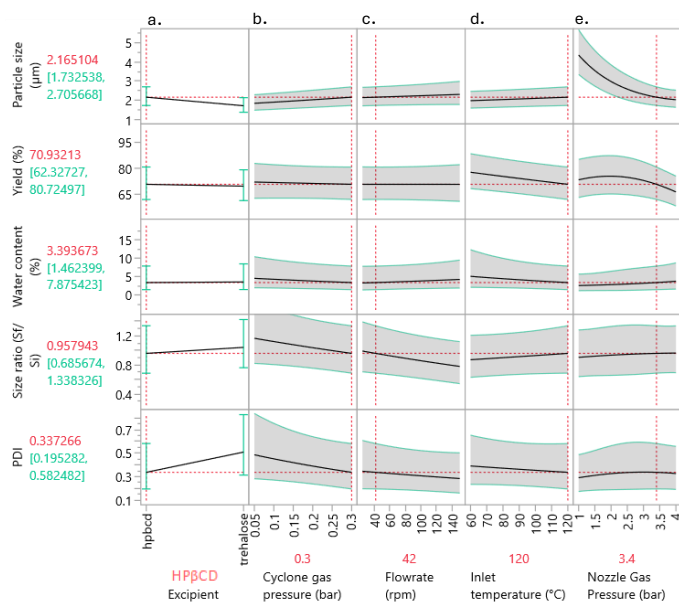
390 3. Results and discussion

391 3.1. DOE_A: Impact of drying parameters and excipient nature on liposome integrity 392 and powder characteristics

393 To better understand the impact of drying parameters and matrix composition on liposome
394 integrity, a first DOE was conducted. Atomization temperature (inlet), feed flow rate (pump
395 speed), atomization nozzle pressure, and cyclone gas flow were each tested at three levels.
396 Two carbohydrate matrices were investigated: trehalose, for its well-established protective
397 effect on liposomes during drying (Lutta et al., 2024; Susa et al., 2021), and HP β CD, for its
398 potential stabilizing effect of liposomes and ability to produce highly aerosolizable, carrier-free
399 powders with favorable morphologies (Dufour et al., 2015; Lechanteur et al., 2022, 2023; Van
400 Den Hoven et al., 2012). Beyond these functional benefits, both carbohydrates, although not
401 approved yet for inhalation, have been reported to exhibit a favorable safety profile for
402 pulmonary administration (Evrard et al., 2004; Iskandar et al., 2021; Zillen et al., 2021). In
403 particular, HP β CD has demonstrated acceptable local tolerability in preclinical inhalation
404 studies and a favorable safety profile in early-phase clinical evaluations (NCT05148312,
405 NCT05000346, NCT04933383). As a starting point, a lipid-to-carbohydrate ratio of 1:99 was
406 chosen.

407 This initial DOE allowed a systematic evaluation of the combined effects of SD parameters and
408 matrix composition on liposome integrity, guiding the development of inhalable powders
409 capable of delivering structurally preserved liposomes. Although the influence of drying
410 parameters on general powder properties is already well established, these properties were
411 included in the DOE to ensure characteristics suitable for pulmonary delivery alongside
412 liposome integrity. All 24 experiments are summarized in Supplementary Data A, which include
413 raw results in terms of SD yield, dry powder particle size, moisture content, as well as liposome
414 size variation and Pdl. These results were used to construct a DOE general profiler (Figure 1),
415 providing initial insight into how these parameters collectively influence powder performance
416 and liposome stability.

Commenté [LB1]: Correct comme ça?



417

418 *Figure 1: DOE_A prediction profiler: Illustration of the effects of carbohydrate type and spray-drying parameters on*
 419 *key powder characteristics and liposome integrity after drying.*

420

421 3.1.1. Impact of spray-drying parameters on liposomal properties

422 Starting with drying parameters, DOE_A analysis revealed a significant combined interaction (p
 423 < 0.05) between flowrate and drying temperature on liposome integrity, particularly influencing
 424 size ratio variation. Specifically, increasing flowrate, directly linked to pump speed, was
 425 associated with reduced liposome size and improved size uniformity, as indicated by a lower
 426 Pdl (Figure 1, column c). Although underexplored in SD, similar trends in microfluidic and
 427 extrusion systems, suggested that shear stress and rapid dispersion from higher flow rates
 428 can reduce liposome size (Ong et al., 2016; Ota et al., 2023).

429 Interestingly, increasing the drying temperature from 60 to 120 °C ($T^{\circ}\text{out}$ ~40 and ~75 °C,
 430 respectively) appeared to improve liposome integrity, as indicated by a lower Pdl and a size
 431 ratio approaching 1 (Figure 1, column d). This may result from faster solvent evaporation,
 432 which limits lipid rearrangement (Dattani et al., 2025), and from the rapid formation of a
 433 protective carbohydrate matrix that stabilizes membranes (Steiner et al., 2022). Importantly,
 434 the combined interaction between flowrate and inlet temperature ($T^{\circ}\text{in}$) suggests a
 435 compensatory mechanism rather than a purely synergistic one. At lower flowrates, atomization
 436 is generally associated with larger droplets formation and longer drying times. However,
 437 increasing the $T^{\circ}\text{in}$ may enhance evaporation kinetics and thereby reduce the duration during
 438 which liposomal membranes are exposed to potentially destabilizing conditions. This balance
 439 is likely to limit lipid rearrangement and support the preservation of liposomal integrity under
 440 conditions combining low flowrate and higher $T^{\circ}\text{in}$. Though moderate for SD processes, a $T^{\circ}\text{in}$
 441 of 120 °C appears to balance liposome stability and generating powders suitable for effective
 442 lung deposition, as supported by findings from recent literature (Khan et al., 2024;
 443 Zimmermann et al., 2022).

444 Furthermore, cyclone and nozzle gas pressure showed no significant effect on liposome
 445 integrity, although higher cyclone pressure tended to reduce size ratio and Pdl, suggesting
 446 improved homogeneity (Figure 1, columns b and e). Additionally, even if increasing nozzle gas
 447 pressure showed minimal impact on liposomes integrity, excessive atomization, especially with
 448 bi-fluid nozzles, may still disrupt lipid vesicle structure via high shear stress, as reported by
 449 recent SD studies on biologics (Poozesh et al., 2025).

450 Overall, significant effects of process parameters are summarized in Supplementary Data B.

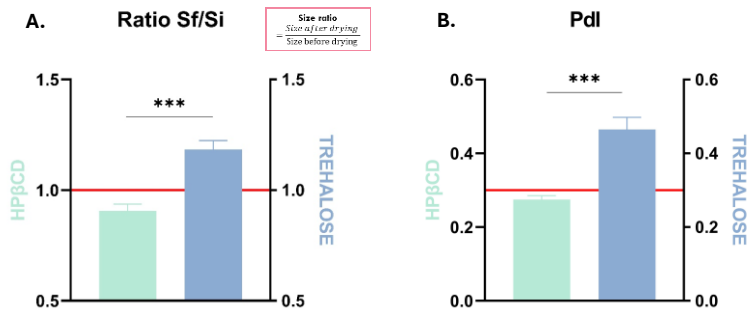
451 3.1.2. Comparative evaluation of trehalose and HPβCD as protective excipients in
 452 liposome spray-drying

453 Having established the influence of drying parameters, the 24-experiment design then
 454 compared the influence of two distinct carbohydrates matrix, HPβCD and trehalose, identifying
 455 one optimal condition for each that balanced powder properties with liposomal stability. These
 456 conditions, reproduced and validated in triplicate, are summarized in Table 1 below.

457 Table 1: Optimal drying conditions for liposomes using HPβCD and trehalose, as determined by DOE_A.

Optimal condition	HPβCD	Trehalose
Inlet temperature (°C)	120	120
Outlet temperature (°C)	~75	~75
Pump speed (rpm)	42	150
Flowrate (g/min)	~1.56	~5.66
Nozzle gas pressure (bar)	3.4	4.0
Cyclone gas pressure (bar)	0.3	0.05

458
 459 Although the DOE analysis indicated that the nature of the excipient had no statistically
 460 significant impact on Pdl values, subsequent validation experiments underscored its practical
 461 importance. While both formulations yielded physically acceptable inhalable powders,
 462 trehalose was associated with a pronounced increase in liposome size upon reconstitution,
 463 exhibiting a size ratio of 1.18 ± 0.04 and a mean Pdl of 0.47 ± 0.03 (Figures 2A–B). These
 464 findings indicate reduced size homogeneity and potential membrane destabilization,
 465 suggesting that the HPβCD-based formulation represents the most favorable condition for
 466 preserving liposome integrity.



467
 468 Figure 2: Effect of carbohydrate type on liposome integrity after spray-drying, as determined by DOE statistical
 469 analysis. Measured size ratios and Pdl values for HPβCD- and trehalose-based formulations under their respective
 470 optimal drying conditions, with prediction intervals indicated. Analyses were performed in triplicates ($n = 3$) and
 471 results are presented as mean \pm standard deviation.

472 Differences in performance can be explained by the distinct stabilization mechanisms of both
 473 protectants. This may first be attributed to differences in the vitrification behavior of both

474 carbohydrate matrix. Indeed, during vitrification, an amorphous glassy matrix forms around the
475 liposomes, physically immobilizing them and thereby limiting membrane rearrangements
476 during dehydration (Grasmeijer et al., 2013). The effectiveness of this process largely depends
477 on the excipient's glass transition temperature (T_g): above this temperature, the matrix softens,
478 loses rigidity, and can no longer effectively protect the vesicles, leading to increased lipid
479 mobility and structural disruption (Ingvarsson et al., 2011; Van Den Hoven et al., 2012). In this
480 study, DSC measurements confirmed T_g consistent with literature values, namely
481 approximately 250 °C for HP β CD and approximately 100 °C for trehalose (Roe & Labuza,
482 2005; Wilhelms et al., 2023; Zheng & Chow, 2009). Consequently, HP β CD remains well above
483 the drying temperatures applied, whereas trehalose operates closer to the outlet temperature
484 (~75 °C), resulting in comparatively weaker stabilization.

485 Beyond vitrification that plays a central role in liposome stabilization during SD, excipients can
486 also stabilize liposomes by forming hydrogen bonds with membrane surfaces during
487 dehydration, replacing water molecules and stabilizing bilayer structure, similar to freeze-
488 drying mechanisms (Ingvarsson et al., 2011). Van den Hoven *et al.* notably reported that
489 HP β CD provides enhances protective effects compared to trehalose on PEGylated liposomes,
490 likely due to its higher density of hydrogen bond donors and acceptors (Van Den Hoven et al.,
491 2012). This feature, supported by its greater number of hydroxyl groups (Hammoud et al.,
492 2019), promotes more efficient membrane stabilization and better preservation of liposome
493 characteristics (Kumar et al., 2020; Yergey et al., 2017).

494 Overall, the protective capacity of HP β CD is reflected in the post-drying liposome
495 characteristics, with preserved size (size ratio = 0.91 ± 0.03) and uniform particle distribution
496 (Pdl = 0.27 ± 0.01), as predicted by the DOE profiler (Figure 1, column a). Importantly, the
497 slightly reduced size ratio (0.91) in combination with a relatively low PDI indicates that the
498 minor decrease in liposomal diameter likely reflects subtle bilayer compaction or hydration
499 changes during drying, rather than any loss of vesicle integrity. Under its optimal conditions
500 (Table 1), the formulation achieved high drying efficiency ($80.46 \pm 4.74\%$), an inhalable particle
501 size of $2.83 \pm 0.24 \mu\text{m}$, and low residual moisture ($4.60 \pm 0.42\%$), ensuring stability and
502 minimizing degradation. Furthermore, powders produced under the optimal DOE_A conditions
503 using HP β CD exhibited sustained liposomal stability over 1 year of storage, as reflected by
504 unchanged liposomal size and Pdl, alongside stable powder water content over time. These
505 long-term stability results are presented in Supplementary C.

506 These results demonstrate that HP β CD supports the production of inhalable liposomal
507 powders with favorable DPI properties and liposomes structural integrity, confirming its
508 suitability as a drying stabilizer for pulmonary delivery. However, optimal liposome preservation
509 was achieved only within a narrow experimental window, highlighting the critical role of a
510 multifactorial DOE approach in identifying precise formulation conditions, as represented by
511 the experimental design space (Supplementary Data D).

512

513 3.1.3. Application of optimized Spray-Drying parameters to budesonide- 514 encapsulated liposomes

515 The optimal condition identified and validated in DOE_A using HP β CD as a protective
516 carbohydrate matrix was applied to liposomes encapsulating BUD, a hydrophobic inhaled
517 corticosteroid (ICS) commonly used in asthma and COPD, to further assess post-drying
518 integrity and drug retention. The transfer study first confirmed the preservation of liposomal
519 size, with pre-drying and post-drying diameters of 125.95 ± 6.15 and 118.20 ± 8.3 nm,
520 respectively, yielding a size ratio of 0.95 ± 0.04 . The produced liposomes exhibited a particle
521 size below 200 nm and a Pdl of 0.229 ± 0.01 , indicating physicochemical properties
522 appropriate for a pulmonary liposomal formulation and the uniformity required for the clinical

523 application of lipid-based nanocarriers (Danaei et al., 2018; Zhang et al., 2025). Furthermore,
524 the zeta potential was measured at -4.46 ± 1.30 mV, indicating a near-neutral surface charge
525 that supports effective mucus penetration and cellular uptake, while minimizing the cytotoxicity
526 typically associated with positively charged liposomes (Lechanteur et al., 2016; Zhang et al.,
527 2025; Zhao et al., 2022).

528 However, despite the preservation of physicochemical properties, post-rehydration dialysis,
529 used to remove free, non-encapsulated drug, revealed that $33.41 \pm 3.64\%$ of BUD was
530 released after drying. This partial loss suggests potential leakage or destabilization of the
531 liposomal membrane during atomization, underscoring the need for further optimization
532 (DOE_B) to improve drug retention.

533

534 3.2. DOEB: Impact of liposome composition and liposome-to-carbohydrate ratios 535 on liposome integrity and powder characteristics

536

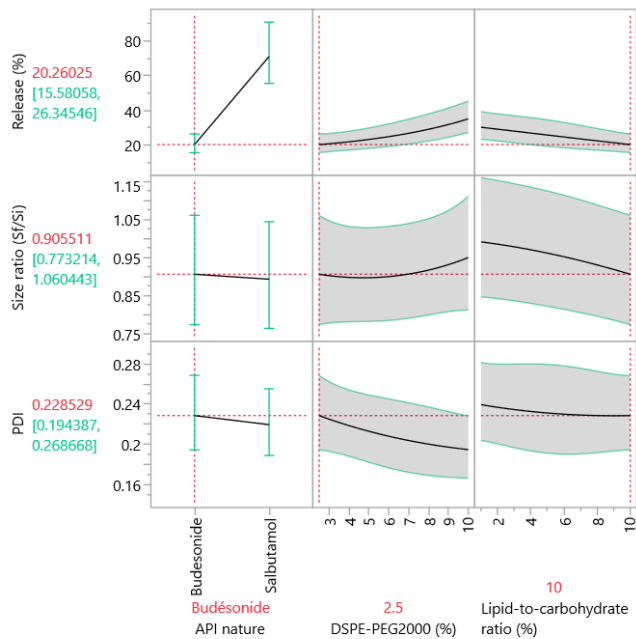
537 Following DOE_A, a second experimental plan evaluated the impact of liposome composition
538 (excipients and API) and liposome-to-carbohydrate ratios on liposome integrity and powder
539 characteristics. Specifically, the effects of the nature of the encapsulated API and the liposome-
540 to-carbohydrate (L/C) ratio were investigated to assess drug retention and the protective role
541 of the carbohydrate matrix while increasing the total liposomal content in the resulting powders.
542 BUD and SAL, a short-acting beta-2 agonist (SABA), were selected as models for hydrophobic
543 and hydrophilic drugs, respectively, along with their prominent use in combination therapies for
544 asthma (LaForce et al., 2025). In addition, the influence of liposomal composition was
545 examined by varying the proportion of DSPE-PEG₂₀₀₀, for its potential steric stabilization of
546 liposomes during SD. Although PEGylated lipids are more extensively characterized in
547 parenteral liposomal products, as exemplified by their use in Doxil[®], they have also been
548 investigated for pulmonary delivery, with preclinical inhalation studies indicating good
549 tolerability and no major toxicological or pharmacokinetic alterations following repeated
550 administration (Bai & Ahsan, 2010; Muralidharan et al., 2014).

551 In all experiments conducted within this design, particle size and residual moisture content
552 were systematically monitored but were not incorporated into the modeling process within the
553 DOE_B framework. The experimental design, along with the corresponding raw data, is provided
554 in Supplementary Data E.

555

556 DOE_B experiments performed with BUD and SAL loaded liposomes revealed that the DPI
557 properties and liposome integrity (size ratio and Pdl) consistently remained within acceptable
558 limits, regardless of API type, lipid composition and quantity. Specifically, all produced powders
559 exhibited a particle size of 2.75 ± 0.50 μ m and a residual moisture content of $3.58 \pm 1.28\%$,
560 values well within the range suitable for inhalation. Moreover, a liposomal size ratio of $0.93 \pm$
561 0.03 and an average Pdl of 0.22 ± 0.02 further confirmed the preservation of liposome integrity
562 after drying. Collectively, these findings highlight that DPI performance and liposome integrity
563 are predominantly governed by SD parameters and carbohydrate matrix type, as identified in
564 DOE_A, whereas the variables examined in DOE_B, although exerting minor effects, still resulted
565 in outcomes meeting the desired specifications. The effects of the tested parameters on
566 liposome integrity and API release are illustrated in the DOE_B profiler (Figure 3), along with a
567 summary of the parameters significantly affecting drug release after drying is presented in
568 Supplementary Data F.

569



570

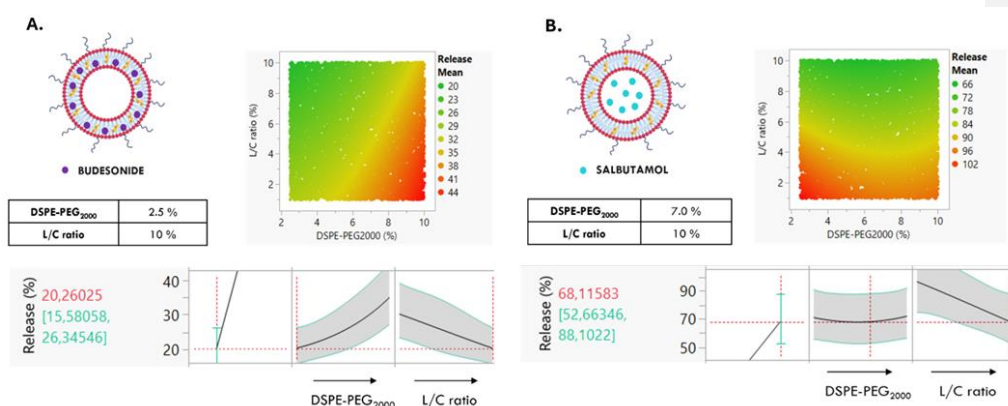
571

572 Figure 3: DOE_B prediction profiler illustrating the influence of API type, DSPE-PEG₂₀₀₀ content, and L/C ratio on
 573 key powder properties and liposome integrity post-drying, with particular emphasis on drug release after drying.
 574 (B) Predicted optimal drying conditions for BUD-loaded liposomes, highlighting the effects of DSPE-PEG₂₀₀₀
 575 content and L/C ratio on BUD release. (C) Predicted optimal drying conditions for SAL-loaded liposomes,
 576 highlighting the effects of DSPE-PEG₂₀₀₀ content and L/C ratio on SAL release.

577 When examining the extent of API release from liposomes during the drying process, the
 578 nature of the encapsulated compound appears to play a critical role. Liposomes loaded with
 579 BUD could exhibit limited release when optimized, stabilizing around 20%, whereas those
 580 encapsulating SAL show significantly higher release levels, reaching approximately 70%
 581 (Figure 3). This imbalance is likely due to structural reorganization of the liposomes during
 582 drying, which promotes leakage from the aqueous core. Given SAL's high water solubility, it
 583 diffuses more readily out of the aqueous heart of the liposome, while BUD, with a stronger
 584 affinity for the lipid bilayer, remains largely retained. Another possible explanation highlighted
 585 by Wessman *et al.* (Wessman *et al.*, 2010), is that cyclodextrin concentration increases during
 586 solvent evaporation, creating an osmotic gradient that may drive the efflux of the internal
 587 aqueous compartment, leading to the selective release of the hydrophilic drug, consistent with
 588 classical osmotic theory. This hypothesis was experimentally excluded (see Figure 6).
 589

590 Importantly, the key finding of DOE_B reveals that an increased percentage of DSPE-PEG₂₀₀₀
 591 in liposomes encapsulating hydrophobic drugs markedly enhances their release during the
 592 drying process, as illustrated by the zoomed section of the profiler corresponding to BUD
 593 optimal condition (Figure 4A). This effect is likely attributable to the combined influence of two
 594 factors: the increased hydrophilicity conferred by the PEGylated lipids at the liposome surface
 595 and the elevated drying temperatures, which together could compromise the structural integrity
 596 of the lipid membrane and increase bilayer fluidity, thereby facilitating the release of the

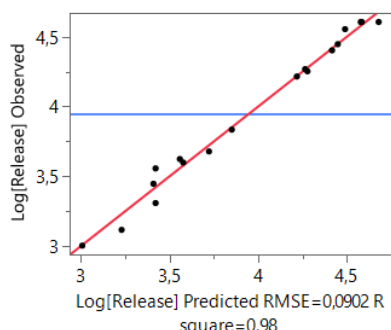
597 entrapped hydrophobic drug (Giakoumatos et al., 2022; Khan et al., 2024). Nevertheless, a
 598 minimal proportion of DSPE-PEG₂₀₀₀ remains essential to prevent vesicle aggregation during
 599 atomization by providing a steric hydrophilic barrier (Li et al., 2015; Tunsirikongkon et al.,
 600 2019). This effect is reflected in the profiler, where an increase in the PEGylated fraction
 601 correlates with a lower Pdl (Figure 3). Additionally, PEGylation offers benefits in the pulmonary
 602 context by enhancing mucus penetration, thereby reducing mucociliary clearance and
 603 extending residence time (Li et al., 2021; Osman et al., 2018). A slight percentage of PEGylated
 604 lipid thus remains essential. In contrast, the release of hydrophilic drugs, which are confined
 605 to the aqueous core of the liposomes, is minimally impacted by variations in DSPE-PEG₂₀₀₀
 606 content (Figure 4B), highlighting the selective influence of PEGylation on drug retention in the
 607 membrane.



608 *Figure 4: (A) Predicted optimal drying conditions for BUD-loaded liposomes, illustrating the influence of DSPE-PEG₂₀₀₀*
 609 *content and lipid-to-carbohydrate (L/C) ratio on BUD release during SD. An increase in DSPE-PEG₂₀₀₀*
 610 *content is associated with enhanced BUD leakage, whereas increasing the L/C ratio results in reduced BUD release, leading to*
 611 *an optimal formulation containing 2.5% DSPE-PEG₂₀₀₀ and an L/C ratio of 10% to minimize BUD loss during drying.*
 612 *(B) Predicted optimal drying conditions for SAL-loaded liposomes, illustrating the influence of DSPE-PEG₂₀₀₀*
 613 *content and L/C ratio on SAL release during SD. While variations in DSPE-PEG₂₀₀₀ content have no significant impact on SAL*
 614 *release, increasing the L/C ratio reduces SAL leakage, resulting in an optimal formulation containing 7% DSPE-PEG₂₀₀₀*
 615 *and an L/C ratio of 10% to limit SAL loss during drying.*

616
 617 Moreover, and notably, despite the influence of PEGylated lipid content, a consistent and
 618 significant ($p < 0.0001$) reduction in drug release is observed for both API-loaded liposome
 619 formulations as the L/C ratio increases (Figures 4A-B). This trend may be attributed to a higher
 620 concentration of liposomes within the atomized liquid, resulting in a greater number of
 621 liposomes within each droplet. Such a configuration likely promotes mutual shielding among
 622 liposomes, particularly those located at the core of the droplet, thereby reducing their direct
 623 exposure to drying stresses. This protective effect contributes to better preservation of
 624 liposomal membrane integrity and limits premature API leakage. Additionally, increasing the
 625 lipid content raises the viscosity of the droplets, potentially slowing API diffusion from
 626 destabilized liposomes during the rapid drying phase. Although still highly hypothetical, these
 627 two combined mechanisms could be responsible for the decreased API release observed after
 628 drying with increasing L/C ratio.

629
 630 Furthermore, Figure 5 shows the correlation between observed and predicted release
 631 percentages. The data closely follows the line of identity (red), indicating a strong agreement
 632 between predicted and measured values. The high R^2 (0.99081), and highly significant p-value
 633 (<0.0001) confirm the excellent predictive performance of the model.



634

635 *Figure 5: Observed (measured) and predicted (via linear regression: solid red line) drug release values for all*
 636 *considered powders.*

637 Ultimately, based on the comprehensive analysis of all measured parameters, optimal
 638 formulations were identified for both BUD (Figure 4A) and SAL-loaded liposomes (Figure 4B)
 639 to minimize drug release during the drying while preserving liposome structural integrity. For
 640 both drugs, the total lipid content was maintained at 10%, with the optimal DSPE-PEG₂₀₀₀
 641 content being 2.5% for BUD and 7% for SAL. These conditions effectively balance drug
 642 retention and liposome stability during drying, thereby ensuring the best preservation of
 643 liposomal properties. Both conditions were validated in triplicate. Furthermore, given the
 644 minimal effect of PEGylated lipid on SAL release and considering the therapeutic interest of
 645 combining an ICS with a SABA in the treatment of asthma, co-encapsulation of both APIs was
 646 subsequently evaluated using the BUD-optimal formulation. All results are presented in Table
 647 4 and fall within the validation ranges predicted by the DOE analysis, confirming their suitability
 648 for inhalation based on particle characteristics, as well as liposome properties and integrity
 649 after drying.

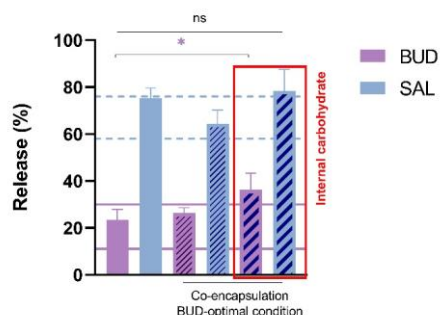
650 *Table 1: Overall results of the validation of the BUD-optimal condition, the SAL-optimal condition, and the BUD-*
 651 *optimal condition applied to liposomes co-encapsulating both APIs. Analyses were performed in triplicates (n = 3) and*
 652 *results are presented as mean ± standard deviation.*

	BUD	SAL	Co-encapsulation	
DPI properties	Drying Yield (%)	75.85 ± 6.77	74.41 ± 2.70	76.03 ± 0.08
	Particle size (µm)	2.79 ± 0.05	2.55 ± 0.03	2.64 ± 0.03
	Water content (%)	4.26 ± 0.77	2.71 ± 0.48	3.50 ± 0.70
Liposomes properties	Liposomes size after powders rehydration (nm)	127.1 ± 6.79	127.43 ± 1.07	128.63 ± 4.21
	Size ratio (Sf/Si)	0.92 ± 0.05	0.96 ± 0.01	0.92 ± 0.01
	Pdl	0.21 ± 0.03	0.21 ± 0.00	0.22 ± 0.01
	ZP (mV)	-2.73 ± 0.39	-2.31 ± 0.25	-2.92 ± 0.08

653

654

655 Regarding the percentage of drug that leaked upon drying, Figure 6 demonstrates that, under
 656 their respective optimal conditions, BUD exhibited drug release value ranging from 11.42 and
 657 30.06%, with a mean drug release of 23.57 ± 4.38%, while SAL ranged from 62 and 76.03%,
 658 with a mean release of 75.38 ± 4.21%, respectively. Moreover, when applying the BUD-optimal
 659 conditions to liposomes co-encapsulating both drugs, the results remained within the validated
 660 ranges, with release values of 26.35 ± 2.24% for BUD and 64.50 ± 4.71% for SAL. These
 661 values fall within the validation limits for both optimal conditions, thereby confirming the
 662 statistical robustness and compliance with this second design.



663

664
665
666
667

Figure 6: Drug release values of BUD- and SAL-loaded liposomes under their respective optimal spray-drying conditions, and for co-encapsulated liposomes processed under BUD-optimal conditions with or without internal carbohydrate incorporation. Analyses were performed in triplicates ($n = 3$) and results are presented as mean \pm standard deviation.

668 Finally, dry liposomal formulations are well known to preserve liposome stability over time
669 (Changsan et al., 2009; Dattani et al., 2025), particularly by maintaining encapsulation
670 efficiency during storage. Initial stability studies on the final formulation, shown in
671 Supplementary Data G, support this concept.

672

673 3.3. Application of the optimized spray-drying process to additional APIs

674 3.3.1. Evaluation of the influence of API hydrophobicity on drug release upon 675 drying

676 To evaluate the transferability and robustness of the combined findings from both DOE studies,
677 the optimized drying parameters and carbohydrate matrix selection identified in DOE_A,
678 together with insights from DOE_B, resumed in Table 5, were applied to additional APIs
679 displaying varying degrees of hydrophobicity. These included formoterol fumarate (FOR),
680 indacaterol maleate (IND), and ciclesonide (CIC). The hydrophobicity of the molecules was
681 determined by their logP values, which reflect the lipophilic character of a drug by measuring
682 its affinity for the octanol phase (Kujawski et al., 2012). The logP values are 0.44, 1.91, 2.42,
683 3.31, and 4.08 for SAL, FOR, BUD, IND, and CIC, respectively (DrugBank, 2025). Beyond
684 their distinct hydrophobicity profiles, these compounds were chosen due to their therapeutic
685 relevance in the management of pulmonary diseases such as asthma and COPD. Additionally,
686 their selection reflects their importance in innovative combination therapies, exemplified by the
687 co-administration of FOR and BUD in the marketed formulation Symbicort[®], as well as
688 emerging dual-molecule strategies involving the co-encapsulation of IND and CIC (Bya et al.,
689 2025). Accordingly, and for therapeutic relevance, liposomes co-encapsulating FOR and BUD,
690 as well as IND and CIC, were prepared, and their performance was compared with that of
691 liposomes co-encapsulating SAL and BUD.

692 Table 5: Overview of the optimized spray-drying (SD) conditions for PEGylated liposomes, combining the SD
693 parameters and carbohydrate selection identified in DOE_A with the lipid composition and lipid-to-carbohydrate ratio
694 determined in DOE_B.

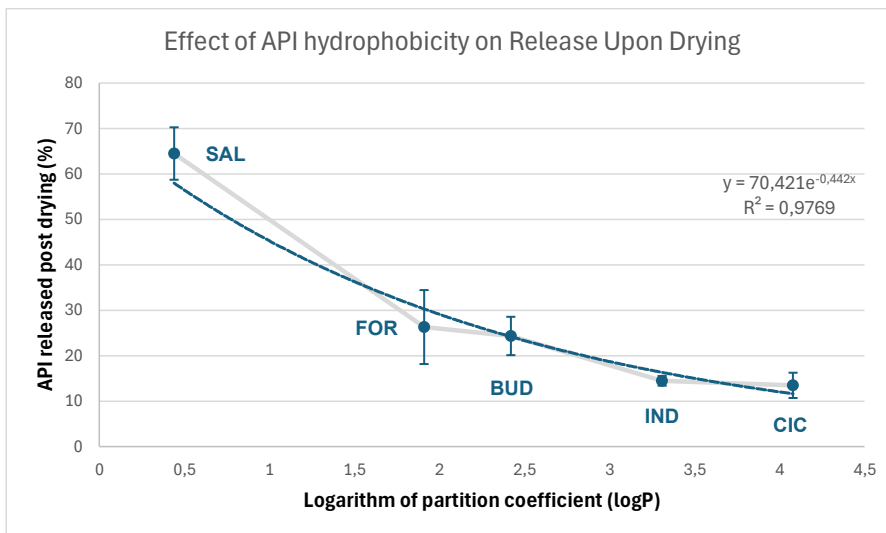
FINAL OPTIMAL CONDITION FOR PEGYLATED DRYING LIPOSOMES

Cyclodextrin matrix	HP β CD
Inlet temperature ($^{\circ}$ C)	120
Outlet temperature ($^{\circ}$ C)	~75

SPRAY-DRYING PROCESS OPTIMAL PARAMETERS (DOE_A)	Pump speed (rpm)	42
	Flowrate (g/min)	~1.56
	Nozzle gas pressure (bar)	3.4
	Cyclone gas pressure (bar)	0.3
LIPOSOMAL OPTIMAL COMPOSITION (DOE_B)	DSPE-PEG ₂₀₀₀ content (%)	2.5
	Lipid-to-carbohydrate ratio (%)	1:9

695

696 Building on this experimental framework, the additional results revealed a notable decrease in
 697 drug release after drying, with measured values of $26.31 \pm 8.13\%$ for FOR, $14.47 \pm 1.07\%$ for
 698 CIC, and $13.47 \pm 2.27\%$ for IND, compared to previous results obtained for BUD and SAL.
 699 When related to their logP values, a clear trend emerges showing that drug release decreases
 700 as lipophilicity increases, supported by a strong exponential correlation ($R^2 = 0.98$) between
 701 API hydrophobicity and release behavior during SD, as initially observed in DOE_B (Figure 7).



702

703 *Figure 7: Influence of API hydrophobicity (log P) on drug release during the spray-drying process under optimized*
 704 *conditions, showing a strong correlation ($R^2 = 0.98$). Analyses were performed in triplicates ($n = 3$) and results are*
 705 *presented as mean.*

706 These findings reinforced those firstly observed in DOE_B, where hydrophobic APIs are better
 707 retained during drying due to their higher affinity for the lipid bilayer, which protects them
 708 despite membrane reorganization. For highly hydrophobic APIs, higher DSPE-PEG₂₀₀₀
 709 contents could be envisaged, as their strong affinity for the lipid bilayer may allow increased
 710 PEGylation without compromising drug retention and potentially improving mucopenetration
 711 (Piñol-Cancer et al., 2025). In contrast, compounds with lower logP exhibited increased
 712 leakage during drying. While the optimized SD process effectively preserved liposomal
 713 integrity, the limited retention of hydrophilic APIs represents a key limitation of this study.
 714 Several formulation strategies reported in the literature may be explored to address this
 715 limitation (Yu et al., 2021), including the use of hydrophobic amino acids (Chen et al., 2012),
 716 polymer coating of liposomes (Altin et al., 2018; Sarabandi & Jafari, 2020), or modulation of
 717 bilayer rigidity through cholesterol enrichment or the use of saturated phospholipids (Anderson
 718 & Omri, 2004; Charnvanich et al., 2010).

719 Accordingly, only liposomes encapsulating relatively hydrophobic APIs were selected for
720 further characterization in the subsequent stages of the project.

721 3.3.2. Characterization of formulated powders and assessment of aerosolization
722 performance

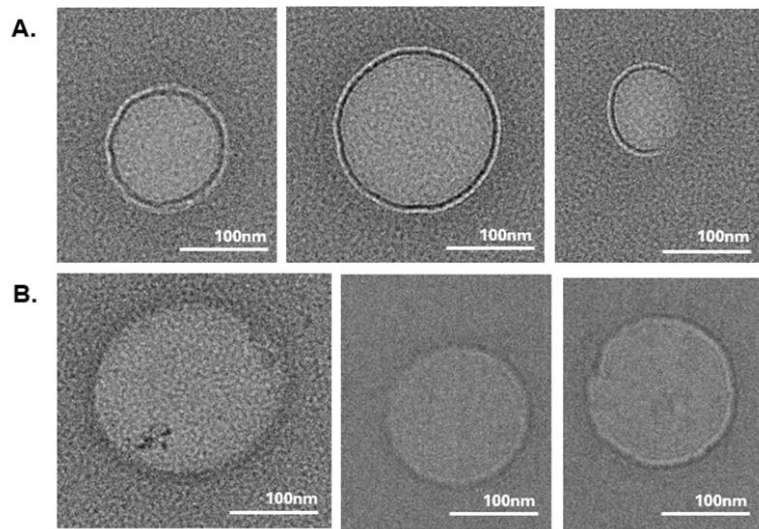
723 Finally, to further characterize the powders obtained under conditions combining both DOEs,
724 additional analyses were conducted to assess API distribution, the morphology of liposomes
725 and dry powder particles, and the lung deposition profile, complementing the previously
726 evaluated powder properties and liposome integrity. These investigations focused on the
727 powders containing liposomes co-encapsulating BUD-FOR and CIC-IND. Powders properties
728 (particle size and water content) and liposomes integrity (size and Pdl) remained consistent
729 with predicted values by DOE_A under optimal conditions, as summarized in Table 5 below.

730 *Table 2: Summary of powder and liposome properties for BUD-FOR and CIC-IND co-encapsulated formulations*
731 *produced under combined DOE-optimized conditions. Analyses were performed in triplicates (n = 3) and results are*
732 *presented as mean ± standard deviation.*

		BUD-FOR	CIC-IND
DPI properties	Drying Yield (%)	72.87 ± 5.50	76.07 ± 0.01
	Particle size (µm)	2.80 ± 0.30	2.79 ± 0.31
	Water content (%)	3.31 ± 0.54	4.84 ± 0.35
Liposomes properties	Liposomes size after powders rehydration (nm)	141.8 ± 7.47	151.83 ± 3.52
	Size ratio (Sf/Si)	0.98 ± 0.03	0.88 ± 0.08
	Pdl	0.23 ± 0.01	0.24 ± 0.02
	ZP (mV)	-2.82 ± 0.14	-2.92 ± 0.32

733

734 To confirm the integrity of the final liposomal formulation under optimal drying conditions,
735 complementary microscopy were performed using both TEM and cryo-TEM. Before
736 atomization, the liposomes exhibited smooth, spherical vesicles with well-defined bilayers
737 (Figures 8A and 9A), a morphology that was preserved after drying, as evidenced by the
738 rehydrated powders displaying structures comparable to the pre-drying liposomes (Figures 8B
739 and 9B). Although the presence of a high carbohydrate content slightly altered bilayer
740 definition, the post-drying liposomes retained their lamellarity and overall morphology,
741 consistent with size estimation. Importantly, TEM and cryo-TEM analyses yielded consistent
742 structural and size observations, providing complementary evidence for the preservation of
743 liposomal integrity after SD. Together, these findings confirm the protective role of HPβCD and
744 highlight the suitability of the optimized drying parameters and liposomal composition for
745 preserving structural integrity.



746
747
748

Figure 8: (A) TEM images of liposomes before SD and (B) rehydrated liposomes after SD, within the rehydrated carbohydrate matrix.

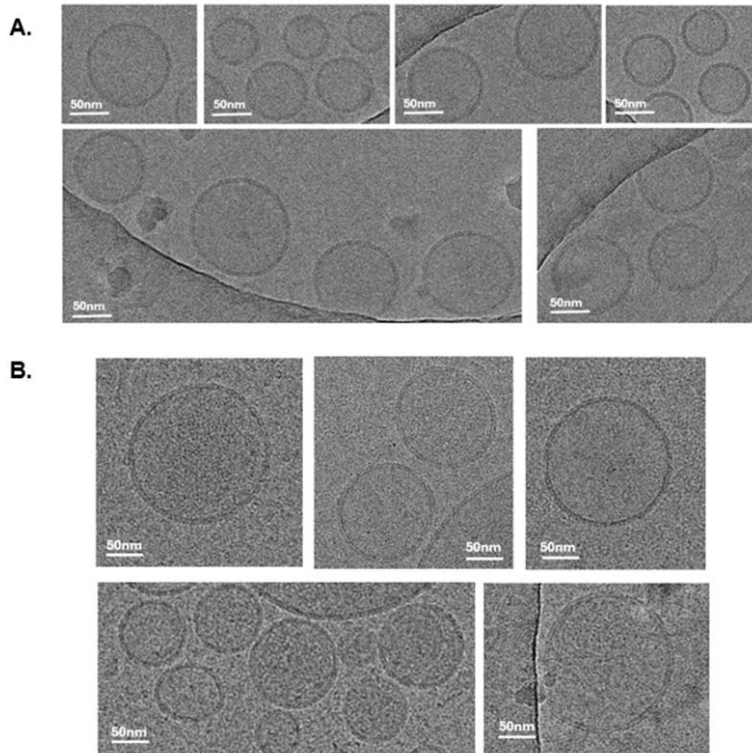


Figure 9: (A) Cryo-TEM images of liposomes before SD and (B) rehydrated liposomes after SD, within the rehydrated carbohydrate matrix.

749
750

751 In the development of DPIs, the therapeutic agent generally constitutes only a minor proportion
 752 of the overall powder mass. This proportion becomes even smaller when the API is
 753 encapsulated in liposomes, as such an approach aims to lower the required dose and thereby
 754 minimize potential adverse effects (Willis et al., 2012). Consequently, a homogeneous
 755 distribution of the API within the resulting powders is essential to ensure consistent therapeutic
 756 performance, with each delivered dose containing the same amount of drug (Marianni et al.,
 757 2021). In this study, powder homogeneity was evaluated by calculating the CV of API content
 758 after drying. As reported by Nguyen *et al.*, API distribution within the powder is generally
 759 deemed acceptable when the CV is below 5% (Nguyen et al., 2015). Analysis of different
 760 samples from the produced powders containing co-encapsulated drug combinations showed
 761 CV values below 5% for all APIs: 1.22 ± 0.42 for FOR, 1.88 ± 1.00 for BUD, 2.17 ± 1.99 for
 762 IND, and $2.69 \pm 1.55\%$ for CIC (Figure 10A). These results confirm a homogeneous distribution
 763 of APIs within the produced powders, reflecting uniform liposome distribution in the droplets
 764 formed during atomization. Moreover, together with the unchanged size and Pdl values, they
 765 indicate that no liposome fusion occurred during the process. Indeed, such fusion could have
 766 resulted in a heterogeneous API distribution in the final powder.

767

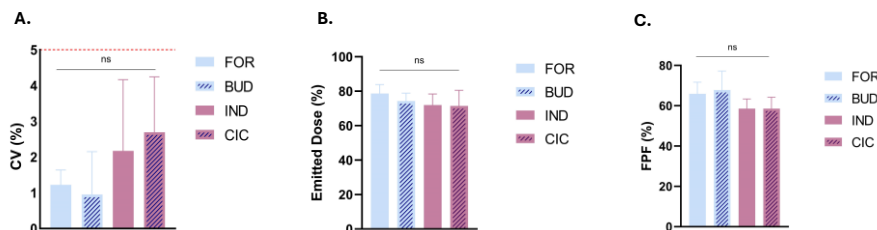


Figure 10: (A) Coefficient of variation of APIs calculated across multiple powder samples, reflecting the uniformity of API distribution within the powders. (B) Emitted Dose (ED) and (C) Fine Particle Fraction (FPF) measured using a Next Generation Impactor (NGI) on powders containing liposomes co-encapsulating FOR–BUD and IND–CIC, at 100L/min. Analyses were performed in triplicates (n = 3) and results are presented as mean ± standard deviation.

768

769
770
771
772

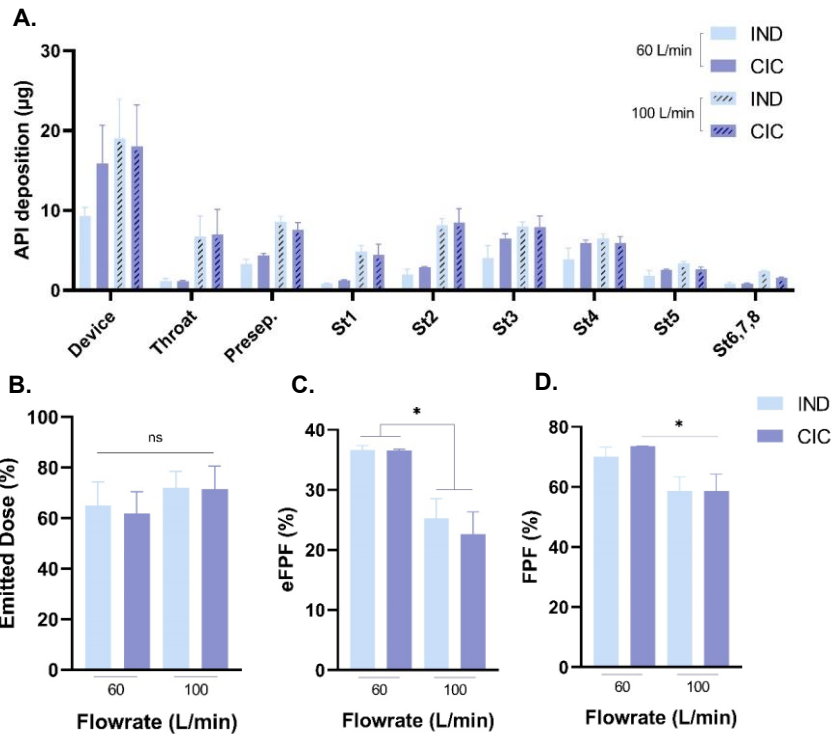
773 Furthermore, the *in vitro* aerodynamic performance of both powders was evaluated using the
774 NGI, with one formulation co-encapsulating FOR and BUD and the other CIC and IND. The
775 BUD-FOR and CIC-IND powders exhibited mass median aerodynamic diameters (MMAD) of
776 $4.19 \pm 1.41 \mu\text{m}$ and $4.60 \pm 0.47 \mu\text{m}$, respectively, with geometric standard deviations (GSD) of
777 1.82 ± 0.05 and 1.83 ± 0.04 , indicating relatively narrow particle size distributions. The SD lipid-
778 based powders exhibited aerodynamic diameters slightly above $3 \mu\text{m}$, which falls within the
779 size range generally considered optimal for deposition in the lower respiratory tract and
780 relevant for treating a wide variety of pulmonary disorders, including asthma and COPD (Ou
781 et al., 2020). Importantly, the particle sizes remained within the recommended 1-5 μm range,
782 allowing efficient lung deposition while minimizing the risks of exhalation or oropharyngeal
783 impaction (Magramane et al., 2023; Zillen et al., 2021). Regarding particle size distribution,
784 although a perfectly monodisperse aerosol would have a GSD close to 1, inhaler-generated
785 powders typically exhibit GSD values around 1.8 (Louey et al., 2004; Mitchell et al., 2003).

786 Among the parameters evaluated, the ED, defined as the fraction of the drug exiting the device,
787 ranged from 75 to 85% for both powders (Figure 10B), considered as high-efficiency DPIs
788 (Behara et al., 2014). Additionally, when calculating the fraction of drug reaching the deepest
789 regions of the lung based on the ED, as characterized by the FPF, all formulations
790 demonstrated efficient pulmonary deposition, with FPF values of $58.54 \pm 4.82\%$ for IND,
791 $58.58 \pm 5.67\%$ for CIC, $63.44 \pm 12.22\%$ for BUD, and $65.87 \pm 5.85\%$ for FOR (Figure 10C).
792 Detailed stage-by-stage deposition data were also generated, showing that all APIs exhibited
793 highly comparable deposition profiles across the NGI stages, thereby indicating consistent
794 aerodynamic behavior throughout the impactor (Supplementary Data H).

795 Furthermore, as COPD predominantly affects the peripheral airways and the lung parenchyma,
796 evaluation of the eFPF represents a more clinically relevant parameter for assessing deep lung
797 delivery (Braidó et al., 2016; Usmani & Barnes, 2012). The eFPF corresponds to the fraction
798 of particles with an aerodynamic diameter below $2 \mu\text{m}$, which are more likely to penetrate and
799 deposit in the small airways and alveolar regions (Hillyer et al., 2018; Usmani et al., 2020). For
800 the tested powders, eFPF values exceeded 20% for all formulations, reaching $23.74 \pm 3.63\%$,
801 $25.35 \pm 0.96\%$, $25.28 \pm 3.23\%$, and $22.68 \pm 3.64\%$ for FOR, BUD, CIC, and IND, respectively.
802 These results are particularly encouraging, as eFPF values above 5% have been widely
803 reported in the literature as indicative of an effective potential for deep lung deposition (Tse et
804 al., 2021).

805 In addition, previous studies indicate that patients using the Breezhaler® typically achieve an
806 inspiratory flow rate of approximately 60 L/min (Abadelah et al., 2018). Therefore, to evaluate
807 aerodynamic performance under clinically relevant conditions, lung deposition experiments

808 were conducted at 60 L/min using the powder encapsulating liposomes co-delivering CIC and
 809 IND.

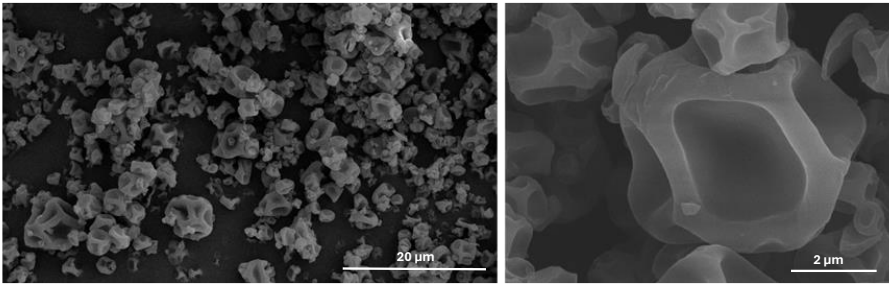


810
 811 *Figure 11: (A) Stage-by-stage deposition profiles, (B) Emittted Dose (ED), (C) extra-Fine Particle Fraction (eFPF) and*
 812 *Fine Particle Fraction (FPF) obtained from NGI lung deposition studies of the optimized powder formulation containing*
 813 *liposomes co-encapsulating CIC and IND at a clinically relevant flow rate of 60 L/min. Results are compared with*
 814 *those obtained at 100 L/min. Analyses were performed in triplicates (n = 3) and results are presented as mean ±*
 815 *standard deviation.*

816 Compared with 100 L/min, powder retention within the inhaler was similar at both flow rates,
 817 as confirmed by the stage-by-stage mass recovery profiles (Figure 11A) and comparable ED
 818 values at 60 L/min with 61.83 ± 8.66% for CIC and 64.98 ± 9.41% for IND (Figure 11B).
 819 Although total deposition across the NGI stages was higher at 100 L/min, increased impaction
 820 in the throat and pre-separator was observed at this flow rate, likely due to enhanced inertial
 821 effects. In contrast, deposition in the respirable fraction remained high at both flow rates, with
 822 eFPF values of 36.58 ± 0.21% and 36.61 ± 0.79% (Figure 11C), and FPF values of 73.55 ±
 823 0.12% and 70.12 ± 0.79% for CIC and IND, respectively (Figure 11D). Notably, both FPF and
 824 eFPF were slightly higher at 60 L/min, suggesting more efficient deep lung delivery under
 825 lower-flow conditions, confirming that the optimized powder formulation retains robust and
 826 clinically relevant aerodynamic performance across physiologically realistic inhalation flow
 827 rates.

828 Overall, these pulmonary deposition results are especially noteworthy given the fixed L/C ratio
829 in the powders and the SD parameters optimized to preserve liposome integrity, especially
830 since higher lipid content has been shown to be associated with a decrease in FPF (Almurshedi
831 et al., 2021). Notably, previous studies on powders composed solely of HP β CD, without
832 liposomes, reported similar FPF values when ultra-fine particles were generated under
833 optimized drying conditions (Bya et al., 2025; Gresse et al., 2024; Santos Gomes et al., 2025).

834 Finally, the morphology of powders obtained under optimal conditions was examined. Despite
835 the presence of a non-negligible fraction of liposomes and drying parameters optimized for
836 liposomal drying, HP β CD-based powders maintained their characteristic deflated structure
837 (Figure 12), which has been previously associated with improved aerodynamic properties and
838 enhanced pulmonary deposition (Dufour et al., 2015; Gresse et al., 2024; Lechanteur et al.,
839 2023).



840
841 *Figure 12: Scanning electron micrographs of spray-dried powders produced under the combined optimal conditions.*

842
843
844
845
846
847
848
849
850
851
852
853
854
855

856 4. Conclusion

857 This study demonstrates that SD of liposomes, when carefully optimized, can produce
858 inhalable powders that maintain liposome structure while exhibiting favorable aerodynamic
859 performance. By combining two scalable, one-step processes, PGSS liposome formation and

860 subsequent SD, robust formulations were achieved even at a high solid content of 5%,
861 highlighting the feasibility of industrial-scale production. Importantly, the use of a systematic
862 DOE approach allowed this work to move beyond formulation-specific outcomes and establish
863 clear relationships between process parameters, formulation attributes, and critical quality
864 attributes relevant to inhalable liposomal products. This integrated, scale-up-oriented strategy
865 provides practical insight into how liposome integrity and DPI performance can be jointly
866 engineered under industrially relevant drying conditions.

867
868 Notably, coupled DOE results demonstrated that HP β CD plays a critical role in protecting
869 liposomes during atomization, while drug retention was primarily influenced by PEGylated lipid
870 content, lipid-to-carbohydrate ratio and API hydrophobicity, with highly hydrophilic compounds
871 exhibiting significant release. Under the optimized conditions, carrier-free powders with a
872 suitable aerodynamic size ($\sim 3 \mu\text{m}$), low residual moisture ($< 5\%$), and high drying yield ($> 75\%$)
873 were obtained. Liposomes retained their structural integrity throughout processing, as
874 confirmed by minimal size variation (ratio 0.9–1.0), mean diameters below 200 nm, narrow
875 size distribution (Pdl ~ 0.2), near-neutral zeta potential, and preservation of their morphology
876 as observed by microscopy. These attributes collectively support efficient pulmonary delivery.

877
878 Optimized formulations co-encapsulating clinically relevant drug combinations
879 (formoterol/budesonide and ciclesonide/indacaterol maleate) further exhibited uniform drug
880 distribution (CV $< 5\%$), characteristic deflated morphology, and efficient aerosolization (eFPF
881 $> 20\%$ and FPF $> 60\%$), underscoring their potential for inhalation therapy. Moreover, the
882 selection of formulation components such as HP β CD, cholesterol, and PEGylated lipids,
883 supported by encouraging preclinical and early clinical experience, reinforces the translational
884 relevance of the proposed approach, while acknowledging that regulatory acceptance for
885 pulmonary delivery must ultimately be addressed in the context of the final product.

886 Taken together, these findings establish a clear framework for designing liposomal dry
887 powders for deep-lung delivery, balancing formulation composition, excipient choice, and
888 process parameters. Ultimately, this work paves the way for the industrial-scale translation of
889 inhalable liposomal therapeutics, demonstrating that a strategic combination of scalable
890 manufacturing methods can reconcile formulation performance with manufacturability.

891 Future investigations, including pharmacokinetic and toxicological evaluation of the final dry
892 powder formulation in an asthmatic rat model using the PreciseInhale[®] system, will be critical
893 to further substantiate the translational potential of combining liposomal encapsulation with
894 carrier-free powder technologies for enhanced pulmonary drug delivery.

CRedit authorship contribution statement

Laure-Anne Bya: Writing – original draft, Writing – review & editing, Investigation, Data curation, Conceptualization. **T. Nghia Dinh**: Data curation, Review. **Noémie Penoy**: Conceptualization, Supervision, review. **Pierre-Yves Sacré**: Conceptualization, Investigation, Review. **Didier Cataldo**: Supervision. **Erika Hendrickx**: Data curation. **Louise Conrard**: Data curation. **Brigitte Evrard**: Supervision. **Anna Lechanteur**: Supervision, Writing – review & editing.

Declaration of interest

The authors declare that they have no known competing financial interests or personal relationships that could have appeared to influence the work reported in this paper.

Acknowledgement

This research was funded by the Walloon Region, SPW-EER, DGO6 – Win2Wal – LNPulmo convention n°2210043. Authors want to thank Aquilon Pharma (Liège, Belgium). Authors also want to thank Raphaël Closset from the GREENnMat (Prof. Rudi Cloots) for the Scanning Electron Microscopy (SEM) analysis.

895

896

897

898

899

900

901

902

903

904

905

906

907

908

909

910

911

912

913 REFERENCES

914 Abadela, M., Chrystyn, H., Bagherisadeghi, G., Abdalla, G., & Larhib, H. (2018). Study of the
915 Emitted Dose After Two Separate Inhalations at Different Inhalation Flow Rates and
916 Volumes and an Assessment of Aerodynamic Characteristics of Indacaterol Onbrez
917 Breezhaler® 150 and 300 µg. *AAPS PharmSciTech*, 19(1), 251–261.
918 <https://doi.org/10.1208/s12249-017-0841-y>

919 Abbassi, M., Nejad Ebrahimi, S., & Rahimi, M. (2025). Optimized spray-drying of zinc sulfate-
920 loaded liposomes: physicochemical characterization and in vitro release assessment.
921 *Scientific Reports*, 15(1). <https://doi.org/10.1038/s41598-025-05948-4>

- 922 Alhajj, N., O'Reilly, N. J., & Cathcart, H. (2021). Designing enhanced spray dried particles for
923 inhalation: A review of the impact of excipients and processing parameters on particle
924 properties. In *Powder Technology* (Vol. 384, pp. 313–331). Elsevier B.V.
925 <https://doi.org/10.1016/j.powtec.2021.02.031>
- 926 Allen, T. M., & Cullis, P. R. (2013). Liposomal drug delivery systems: From concept to clinical
927 applications. In *Advanced Drug Delivery Reviews* (Vol. 65, Number 1, pp. 36–48).
928 <https://doi.org/10.1016/j.addr.2012.09.037>
- 929 Almurshedi, A. S., Aljunaidel, H. A., Alquadeib, B., Aldosari, B. N., Alfagih, I. M., Almarshidy, S.
930 S., Eltahir, E. K. D., & Mohamoud, A. Z. (2021). Development of inhalable nanostructured
931 lipid carriers for ciprofloxacin for noncystic fibrosis bronchiectasis treatment. *International*
932 *Journal of Nanomedicine*, 16, 2405–2417. <https://doi.org/10.2147/IJN.S286896>
- 933 Altin, G., Gültekin-Özgüven, M., & Ozcelik, B. (2018). Chitosan coated liposome dispersions
934 loaded with cacao hull waste extract: Effect of spray drying on physico-chemical stability
935 and in vitro bioaccessibility. *Journal of Food Engineering*, 223, 91–98.
936 <https://doi.org/10.1016/j.jfoodeng.2017.12.005>
- 937 Anderson, M., & Omri, A. (2004). The Effect of Different Lipid Components on the in Vitro
938 Stability and Release Kinetics of Liposome Formulations. *Drug Delivery: Journal of*
939 *Delivery and Targeting of Therapeutic Agents*, 11(1), 33–39.
940 <https://doi.org/10.1080/10717540490265243>
- 941 Bai, S., & Ahsan, F. (2010). Inhalable liposomes of low molecular weight heparin for the
942 treatment of venous thromboembolism. *Journal of Pharmaceutical Sciences*, 99(11),
943 4554–4564. <https://doi.org/10.1002/jps.22160>
- 944 Bashyal, S., Suwal, N., Thapa, R., Bagale, L. R., Sugandhi, V. V., Subedi, S., Idrees, S., Panth,
945 N., Elwakil, B. H., El-Khatib, M., Dua, K., & Paudel, K. R. (2025). Liposomal drug delivery
946 system for lung diseases: Recent advancement and future perspectives. In
947 *Nanomedicine: Nanotechnology, Biology, and Medicine* (Vol. 69). Elsevier Inc.
948 <https://doi.org/10.1016/j.nano.2025.102855>
- 949 Behara, S. R. B., Longest, P. W., Farkas, D. R., & Hindle, M. (2014). Development and
950 comparison of new high-efficiency dry powder inhalers for carrier-free formulations.
951 *Journal of Pharmaceutical Sciences*, 103(2), 465–477. <https://doi.org/10.1002/jps.23775>
- 952 Braido, F., Scichilone, N., Lavorini, F., Usmani, O. S., Dubuske, L., Boulet, L. P., Mosges, R.,
953 Nunes, C., Sanchez-Borges, M., Ansotegui, I. J., Ebisawa, M., Levi-Schaffer, F.,
954 Rosenwasser, L. J., Bousquet, J., Zuberbier, T., Canonica, G. W., Cruz, A., Yanez, A.,
955 Yorgancioglu, A., ... Zhang, L. (2016). Manifesto on small airway involvement and
956 management in asthma and chronic obstructive pulmonary disease: an Interasma (Global
957 Asthma Association - GAA) and World Allergy Organization (WAO) document endorsed
958 by Allergic Rhinitis and its Impact on Asthma (ARIA) and Global Allergy and Asthma
959 European Network (GA2LEN). *World Allergy Organization Journal*, 9(1), 1–6.
960 <https://doi.org/10.1186/s40413-016-0123-2>
- 961 Bya, L. A., Bottero, B., Coeurderoi, A., Dinh, T. N., Sacré, P. Y., Ziemons, E., Cataldo, D., Piel,
962 G., Evrard, B., & Lechanteur, A. (2025). Formulation of a dry powder for inhalation
963 combining ciclesonide and indacaterol maleate using spray drying. *International Journal*
964 *of Pharmaceutics*, 678. <https://doi.org/10.1016/j.ijpharm.2025.125696>
- 965 Chang, R. Y. K., Kwok, P. C. L., Khanal, D., Morales, S., Kutter, E., Li, J., & Chan, H. K. (2020).
966 Inhalable bacteriophage powders: Glass transition temperature and bioactivity

- 967 stabilization. *Bioengineering and Translational Medicine*, 5(2).
968 <https://doi.org/10.1002/btm2.10159>
- 969 Changsan, N., Chan, H. K., Separovic, F., & Srichana, T. (2009). Physicochemical
970 characterization and stability of rifampicin liposome dry powder formulations for
971 inhalation. *Journal of Pharmaceutical Sciences*, 98(2), 628–639.
972 <https://doi.org/10.1002/jps.21441>
- 973 Charnvanich, D., Vardhanabhuti, N., & Kulvanich, P. (2010). Effect of cholesterol on the
974 properties of spray-dried lysozyme-loaded liposomal powders. *AAPS PharmSciTech*,
975 11(2), 832–842. <https://doi.org/10.1208/s12249-010-9442-8>
- 976 Chaurasiya, B., & Zhao, Y. Y. (2021). Dry powder for pulmonary delivery: A comprehensive
977 review. In *Pharmaceutics* (Vol. 13, Number 1, pp. 1–28). MDPI AG.
978 <https://doi.org/10.3390/pharmaceutics13010031>
- 979 Chen, K. H., Mueannoom, W., Gaisford, S., & Kett, V. L. (2012). Investigation into the effect of
980 varying l-leucine concentration on the product characteristics of spray-dried liposome
981 powders. *Journal of Pharmacy and Pharmacology*, 64(10), 1412–1424.
982 <https://doi.org/10.1111/j.2042-7158.2012.01521.x>
- 983 Cipolla, D., Gonda, I., & Chan, H. K. (2013). Liposomal formulations for inhalation. In
984 *Therapeutic Delivery* (Vol. 4, Number 8, pp. 1047–1072). Newlands Press Ltd.
985 <https://doi.org/10.4155/tde.13.71>
- 986 Dal Negro, R. W. (2015). Dry powder inhalers and the right things to remember: A concept
987 review. In *Multidisciplinary Respiratory Medicine* (Vol. 10, Number 1). BioMed Central Ltd.
988 <https://doi.org/10.1186/s40248-015-0012-5>
- 989 Danaei, M., Dehghankhold, M., Ataei, S., Hasanzadeh Davarani, F., Javanmard, R., Dokhani,
990 A., Khorasani, S., & Mozafari, M. R. (2018). Impact of particle size and polydispersity
991 index on the clinical applications of lipidic nanocarrier systems. In *Pharmaceutics* (Vol.
992 10, Number 2). MDPI AG. <https://doi.org/10.3390/pharmaceutics10020057>
- 993 Dattani, S., Li, X., Lampa, C., Barriscale, A., Damadzadeh, B., Lechuga-Ballesteros, D., &
994 Jasti, B. R. (2025). Development of Spray-Dried Micelles, Liposomes, and Solid Lipid
995 Nanoparticles for Enhanced Stability. *Pharmaceutics*, 17(1).
996 <https://doi.org/10.3390/pharmaceutics17010122>
- 997 Delma, K. L., Penoy, N., Sakira, A. K., Egrek, S., Sacheli, R., Grignard, B., Hayette, M. P., Issa
998 Somé, T., Evrard, B., Semdé, R., & Piel, G. (2023). Use of supercritical CO₂ for the
999 sterilization of liposomes: Study of the influence of sterilization conditions on the chemical
1000 and physical stability of phospholipids and liposomes. *European Journal of*
1001 *Pharmaceutics and Biopharmaceutics*, 183, 112–118.
1002 <https://doi.org/10.1016/j.ejpb.2023.01.002>
- 1003 DrugBank. (2025). *DrugBank Online*. <https://go.drugbank.com/drugs/DB01001>
- 1004 Dufour, G., Bigazzi, W., Wong, N., Boschini, F., De Tullio, P., Piel, G., Cataldo, D., & Evrard, B.
1005 (2015). Interest of cyclodextrins in spray-dried microparticles formulation for sustained
1006 pulmonary delivery of budesonide. *International Journal of Pharmaceutics*, 495(2), 869–
1007 878. <https://doi.org/10.1016/j.ijpharm.2015.09.052>
- 1008 Eloy, J. O., Claro de Souza, M., Petrilli, R., Barcellos, J. P. A., Lee, R. J., & Marchetti, J. M.
1009 (2014). Liposomes as carriers of hydrophilic small molecule drugs: Strategies to enhance

1010 encapsulation and delivery. In *Colloids and Surfaces B: Biointerfaces* (Vol. 123, pp. 345–
1011 363). Elsevier. <https://doi.org/10.1016/j.colsurfb.2014.09.029>

1012 Evrard, B., Bertholet, P., Gueders, M., Flament, M. P., Piel, G., Delattre, L., Gayot, A., Leterme,
1013 P., Foidart, J. M., & Cataldo, D. (2004). Cyclodextrins as a potential carrier in drug
1014 nebulization. *Journal of Controlled Release*, 96(3), 403–410.
1015 <https://doi.org/10.1016/j.jconrel.2004.02.010>

1016 Furst, T., Dakwar, G. R., Zagato, E., Lechanteur, A., Remaut, K., Evrard, B., Braeckmans, K.,
1017 & Piel, G. (2016). Freeze-dried mucoadhesive polymeric system containing pegylated
1018 lipoplexes: Towards a vaginal sustained released system for siRNA. *Journal of Controlled*
1019 *Release*, 236, 68–78. <https://doi.org/10.1016/j.jconrel.2016.06.028>

1020 Giakoumatos, E. C., Gascoigne, L., Gumí-Audenis, B., García, Á. G., Tuinier, R., & Voets, I. K.
1021 (2022). Impact of poly(ethylene glycol) functionalized lipids on ordering and fluidity of
1022 colloid supported lipid bilayers. *Soft Matter*, 18(39), 7569–7578.
1023 <https://doi.org/10.1039/d2sm00806h>

1024 Goldbach, P., Brochart, H., & Stamm, A. (1993). SPRAY-DRYING OF LIPOSOMES FOR A
1025 PULMONARY ADMINISTRATION. I. CHEMICAL STABILITY OF PHOSPHOLIPIDS. In
1026 *DRUG DEVELOPMENT AND INDUSTRIAL PHARMACY* (Vol. 19, Number 19).

1027 Grasmeijer, N., Stankovic, M., De Waard, H., Frijlink, H. W., & Hinrichs, W. L. J. (2013).
1028 Unraveling protein stabilization mechanisms: Vitrification and water replacement in a
1029 glass transition temperature controlled system. *Biochimica et Biophysica Acta - Proteins*
1030 *and Proteomics*, 1834(4), 763–769. <https://doi.org/10.1016/j.bbapap.2013.01.020>

1031 Gresse, E., Rousseau, J., Akdim, M., du Bois, A., Lechanteur, A., & Evrard, B. (2024).
1032 Enhancement of inhaled micronized powder flow properties for accurate capsules filling.
1033 *Powder Technology*, 437, 119576. <https://doi.org/10.1016/j.powtec.2024.119576>

1034 Haeuser, C., Goldbach, P., Huwyler, J., Friess, W., & Allmendinger, A. (2019). Be aggressive!
1035 amorphous excipients enabling single-step freeze-drying of monoclonal antibody
1036 formulations. *Pharmaceutics*, 11(11). <https://doi.org/10.3390/pharmaceutics11110616>

1037 Hammoud, Z., Khreich, N., Auezova, L., Fourmentin, S., Elaissari, A., & Greige-Gerges, H.
1038 (2019). Cyclodextrin-membrane interaction in drug delivery and membrane structure
1039 maintenance. In *International Journal of Pharmaceutics* (Vol. 564, pp. 59–76). Elsevier
1040 B.V. <https://doi.org/10.1016/j.ijpharm.2019.03.063>

1041 Hillyer, E. V., Price, D. B., Chrystyn, H., Martin, R. J., Israel, E., van Aalderen, W. M. C., Papi,
1042 A., Usmani, O. S., & Roche, N. (2018). Harmonizing the Nomenclature for Therapeutic
1043 Aerosol Particle Size: A Proposal. In *Journal of aerosol medicine and pulmonary drug*
1044 *delivery* (Vol. 31, Number 2, pp. 111–113). NLM (Medline).
1045 <https://doi.org/10.1089/jamp.2017.1396>

1046 Ingvarsson, P. T., Yang, M., Nielsen, H. M., Rantanen, J., & Foged, C. (2011). Stabilization of
1047 liposomes during drying. In *Expert Opinion on Drug Delivery* (Vol. 8, Number 3, pp. 375–
1048 388). <https://doi.org/10.1517/17425247.2011.553219>

1049 Iskandar, A. R., Kolli, A. R., Giralt, A., Neau, L., Fatarova, M., Kondylis, A., Torres, L. O.,
1050 Majeed, S., Merg, C., Corciulo, M., Trivedi, K., Guedj, E., Frentzel, S., Calvino, F., Guy, P.
1051 A., Ivanov, N. V., Peitsch, M. C., & Hoeng, J. (2021). Assessment of in vitro kinetics and
1052 biological impact of nebulized trehalose on human bronchial epithelium. *Food and*
1053 *Chemical Toxicology*, 157. <https://doi.org/10.1016/j.fct.2021.112577>

- 1054 Kaialy, W., & Nokhodchi, A. (2013). Freeze-dried mannitol for superior pulmonary drug delivery
1055 via dry powder inhaler. *Pharmaceutical Research*, 30(2), 458–477.
1056 <https://doi.org/10.1007/s11095-012-0892-4>
- 1057 Khan, I., Edes, K., Alsaadi, I., Al-Khaial, M. Q., Bnyan, R., Khan, S. A., Sadozai, S. K., Khan,
1058 W., & Yousaf, S. (2024). Investigation of Spray Drying Parameters to Formulate Novel
1059 Spray-Dried Proliposome Powder Formulations Followed by Their Aerosolization
1060 Performance. *Pharmaceutics*, 16(12). <https://doi.org/10.3390/pharmaceutics16121541>
- 1061 Kujawski, J., Bernard, M. K., Janusz, A., & Kuźma, W. (2012). Prediction of log P: ALOGPS
1062 application in medicinal chemistry education. *Journal of Chemical Education*, 89(1), 64–
1063 67. <https://doi.org/10.1021/ed100444h>
- 1064 Kumar, A., Cincotti, A., & Aparicio, S. (2020). A theoretical study on trehalose + water mixtures
1065 for dry preservation purposes. *Molecules*, 25(6).
1066 <https://doi.org/10.3390/molecules25061435>
- 1067 LaForce, C., Albers, F., Danilewicz, A., Jeynes-Ellis, A., Kraft, M., Panettieri, R. A., Rees, R.,
1068 Bardsley, S., Dunsire, L., Harrison, T., Sobande, O., Surujbally, R., Trudo, F., Cappelletti,
1069 C., Papi, A., Beasley, R., Chipps, B. E., Israel, E., Pandya, H., ... Bacharier, L. B. (2025).
1070 As-Needed Albuterol–Budesonide in Mild Asthma. *New England Journal of Medicine*,
1071 393(2), 113–124. <https://doi.org/10.1056/nejmoa2504544>
- 1072 Lechanteur, A., & Evrard, B. (2020). Influence of composition and spray-drying process
1073 parameters on carrier-free DPI properties and behaviors in the lung: A review.
1074 *Pharmaceutics*, 12(1). <https://doi.org/10.3390/pharmaceutics12010055>
- 1075 Lechanteur, A., Furst, T., Evrard, B., Delvenne, P., Hubert, P., & Piel, G. (2016). PEGylation of
1076 lipoplexes: The right balance between cytotoxicity and siRNA effectiveness. *European
1077 Journal of Pharmaceutical Sciences*, 93, 493–503.
1078 <https://doi.org/10.1016/j.ejps.2016.08.058>
- 1079 Lechanteur, A., Gresse, E., Orozco, L., Plougouven, E., Léonard, A., Vandewalle, N., Lumay,
1080 G., & Evrard, B. (2023). Inhalation powder development without carrier: How to engineer
1081 ultra-flying microparticles? *Eur J Pharm Biopharm*, 191, 26–35.
1082 <https://doi.org/10.1016/j.ejpb.2023.08.010>
- 1083 Lechanteur, A., Plougouven, E., Orozco, L., Lumay, G., Vandewalle, N., Léonard, A., & Evrard,
1084 B. (2022). Engineered-inhaled particles: Influence of carbohydrates excipients nature on
1085 powder properties and behavior. *International Journal of Pharmaceutics*, 613.
1086 <https://doi.org/10.1016/j.ijpharm.2021.121319>
- 1087 Li, J., Wang, X., Zhang, T., Wang, C., Huang, Z., Luo, X., & Deng, Y. (2015). A review on
1088 phospholipids and their main applications in drug delivery systems. In *Asian Journal of
1089 Pharmaceutical Sciences* (Vol. 10, Number 2, pp. 81–98). Shenyang Pharmaceutical
1090 University. <https://doi.org/10.1016/j.ajps.2014.09.004>
- 1091 Li, J., Zheng, H., Xu, E. Y., Moehwald, M., Chen, L., Zhang, X., & Mao, S. (2021). Inhalable
1092 PLGA microspheres: Tunable lung retention and systemic exposure via polyethylene
1093 glycol modification. *Acta Biomaterialia*, 123, 325–334.
1094 <https://doi.org/10.1016/j.actbio.2020.12.061>
- 1095 Lin, K. C., Lin, H. Y., Yang, C. Y., Chu, Y. L., Xie, R. H., Wang, C. M., Tseng, Y. L., Chen, H.,
1096 Chung, J. H. Y., Yang, J. W., & Chen, G. Y. (2025). Inhalable Mucociliary-On-Chip System

- 1097 Revealing Pulmonary Clearance Dynamics in Nanodrug Delivery. *ACS Nano*, 19(2),
1098 2228–2244. <https://doi.org/10.1021/acsnano.4c11693>
- 1099 Louey, M. D., Van Oort, M., & Hickey, A. J. (2004). *Aerosol Dispersion of Respirable Particles
1100 in Narrow Size Distributions Using Drug-Alone and Lactose-Blend Formulations*.
- 1101 Lutta, A., Knopp, M. M., Tollemeto, M., Pedersen, G. K., Schmidt, S. T., Grohgan, H., & Hagner
1102 Nielsen, L. (2024). The interplay between trehalose and dextran as spray drying
1103 precursors for cationic liposomes. *International Journal of Pharmaceutics*, 652.
1104 <https://doi.org/10.1016/j.ijpharm.2024.123798>
- 1105 Magramane, S., Vlahović, K., Gordon, P., Kállai-Szabó, N., Zelkó, R., Antal, I., & Farkas, D.
1106 (2023). Inhalation Dosage Forms: A Focus on Dry Powder Inhalers and Their
1107 Advancements. In *Pharmaceutics* (Vol. 16, Number 12). Multidisciplinary Digital
1108 Publishing Institute (MDPI). <https://doi.org/10.3390/ph16121658>
- 1109 Marianni, B., Polonini, H., & Oliveira, M. A. L. (2021). Ensuring homogeneity in powder mixtures
1110 for pharmaceuticals and dietary supplements: Evaluation of a 3-axis mixing equipment.
1111 *Pharmaceutics*, 13(4). <https://doi.org/10.3390/pharmaceutics13040563>
- 1112 Meenach, S. A., Anderson, K. W., Zach Hilt, J., McGarry, R. C., & Mansour, H. M. (2013).
1113 Characterization and aerosol dispersion performance of advanced spray-dried
1114 chemotherapeutic PEGylated phospholipid particles for dry powder inhalation delivery in
1115 lung cancer. *European Journal of Pharmaceutical Sciences*, 49(4), 699–711.
1116 <https://doi.org/10.1016/j.ejps.2013.05.012>
- 1117 Milani, S., Faghihi, H., Roulholamini Najafabadi, A., Amini, M., Montazeri, H., & Vatanara, A.
1118 (2020). Hydroxypropyl beta cyclodextrin: a water-replacement agent or a surfactant upon
1119 spray freeze-drying of IgG with enhanced stability and aerosolization. *Drug Development
1120 and Industrial Pharmacy*, 46(3), 403–411.
1121 <https://doi.org/10.1080/03639045.2020.1724131>
- 1122 Mitchell, J. P., Nagel, M. W., Wiersema, K. J., & Doyle, C. C. (2003). Aerodynamic Particle Size
1123 Analysis of Aerosols from Pressurized Metered-Dose Inhalers: Comparison of Andersen
1124 8-Stage Cascade Impactor, Next Generation Pharmaceutical Impactor, and Model 3321
1125 Aerodynamic Particle Sizer Aerosol Spectrometer. In *AAPS PharmSciTech* (Vol. 4,
1126 Number 4). <http://www.aapspharmscitech.org>
- 1127 Muralidharan, P., Mallory, E., Malapit, M., Don, H., & Mansour, H. M. (2014). Inhalable
1128 PEGylated phospholipid nanocarriers and PEGylated therapeutics for respiratory delivery
1129 as aerosolized colloidal dispersions and dry powder inhalers. In *Pharmaceutics* (Vol. 6,
1130 Number 2, pp. 333–353). MDPI AG. <https://doi.org/10.3390/pharmaceutics6020333>
- 1131 Negi, A., Nimbkar, S., & Moses, J. A. (2023). Engineering Inhalable Therapeutic Particles:
1132 Conventional and Emerging Approaches. In *Pharmaceutics* (Vol. 15, Number 12).
1133 Multidisciplinary Digital Publishing Institute (MDPI).
1134 <https://doi.org/10.3390/pharmaceutics15122706>
- 1135 Nguyen, D., Rasmuson, A., Björn, I. N., & Thalberg, K. (2015). Mechanistic time scales in
1136 adhesive mixing investigated by dry particle sizing. *Eur J Pharm Biopharm*, 69, 19–25.
1137 <https://doi.org/10.1016/j.ejps.2014.12.016>
- 1138 Nugraheni, R. W., Setyawan, D., & Yusuf, H. (2017). Physical characteristics of liposomal
1139 formulation dispersed in HPMC matrix and freeze-dried using maltodextrin and mannitol

1140 as lyoprotectant. *Pharmaceutical Sciences*, 24(4), 285–292.
1141 <https://doi.org/10.15171/PS.2017.42>

1142 Ong, S. G. M., Chitneni, M., Lee, K. S., Ming, L. C., & Yuen, K. H. (2016). Evaluation of
1143 extrusion technique for nanosizing liposomes. *Pharmaceutics*, 8(4).
1144 <https://doi.org/10.3390/pharmaceutics8040036>

1145 Osman, G., Rodriguez, J., Chan, S. Y., Chisholm, J., Duncan, G., Kim, N., Tatler, A. L.,
1146 Shakesheff, K. M., Hanes, J., Suk, J. S., & Dixon, J. E. (2018). PEGylated enhanced cell
1147 penetrating peptide nanoparticles for lung gene therapy. *Journal of Controlled Release*,
1148 285, 35–45. <https://doi.org/10.1016/j.jconrel.2018.07.001>

1149 Ota, A., Mochizuki, A., Sou, K., & Takeoka, S. (2023). Evaluation of a static mixer as a new
1150 microfluidic method for liposome formulation. *Frontiers in Bioengineering and*
1151 *Biotechnology*, 11. <https://doi.org/10.3389/fbioe.2023.1229829>

1152 Ou, C., Hang, J., & Deng, Q. (2020). Particle deposition in human lung airways: Effects of
1153 airflow, particle size, and mechanisms. *Aerosol and Air Quality Research*, 20(12), 2846–
1154 2858. <https://doi.org/10.4209/aaqr.2020.02.0067>

1155 Pasero, L., Susa, F., Limongi, T., & Pisano, R. (2024). A Review on Micro and Nanoengineering
1156 in Powder-Based Pulmonary Drug Delivery. In *International Journal of Pharmaceutics*
1157 (Vol. 659). Elsevier B.V. <https://doi.org/10.1016/j.ijpharm.2024.124248>

1158 Penoy, N., Delma, K. L., Tonakpon, H. A., Grignard, B., Evrard, B., & Piel, G. (2022). An
1159 innovative one step green supercritical CO₂ process for the production of liposomes co-
1160 encapsulating both a hydrophobic and a hydrophilic compound for pulmonary
1161 administration. *International Journal of Pharmaceutics*, 627.
1162 <https://doi.org/10.1016/j.ijpharm.2022.122212>

1163 Penoy, N., Grignard, B., Evrard, B., & Piel, G. (2021). A supercritical fluid technology for
1164 liposome production and comparison with the film hydration method. *International Journal*
1165 *of Pharmaceutics*, 592. <https://doi.org/10.1016/j.ijpharm.2020.120093>

1166 Piñol-Cancer, M., Fernández-Méndez, L., Carrillo-Romero, J., Urkola-Arsuaga, A., Azkargorta,
1167 M., Elortza, F., Gofii-de-Cerio, F., García-Mouton, C., de Alejo, C. M. P., Ismalaj, E.,
1168 Cañadas, O., Pérez-Gil, J., Ruíz-Cabello, J., & Carregal-Romero, S. (2025). The role of
1169 PEGylation in the pulmonary delivery of antifibrotic liposomal therapies. *Journal of*
1170 *Controlled Release*, 386. <https://doi.org/10.1016/j.jconrel.2025.114134>

1171 Poozesh, S., Connaughton, P., Sides, S., Lechuga-Ballesteros, D., Patel, S. M., & Manikwar,
1172 P. (2025). Spray drying process challenges and considerations for inhaled biologics. In
1173 *Journal of Pharmaceutical Sciences* (Vol. 114, Number 2, pp. 766–781). Elsevier B.V.
1174 <https://doi.org/10.1016/j.xphs.2024.11.028>

1175 Roe, K. D., & Labuza, T. P. (2005). Glass transition and crystallization of amorphous trehalose-
1176 sucrose mixtures. *International Journal of Food Properties*, 8(3), 559–574.
1177 <https://doi.org/10.1080/10942910500269824>

1178 Rudokas, M., Najlah, M., Alhnan, M. A., & Elhissi, A. (2016). Liposome Delivery Systems for
1179 Inhalation: A Critical Review Highlighting Formulation Issues and Anticancer Applications.
1180 *Medical Principles and Practice*, 25(2), 60–72. <https://doi.org/10.1159/000445116>

1181 Safaeian Laein, S., Samborska, K., Can Karaca, A., Mostashari, P., Akbarbaglu, Z., Sarabandi,
1182 K., & Jafari, S. M. (2024). Strategies for further stabilization of lipid-based delivery

1183 systems with a focus on solidification by spray-drying. *Trends in Food Science &*
1184 *Technology*, 146, 104412. <https://doi.org/10.1016/j.tifs.2024.104412>

1185 Santos Gomes, B. F., Bya, L. A., Koch, N., Cabral-Marques, H., Evrard, B., & Lechanteur, A.
1186 (2025). Cannabidiol and Hydroxypropyl- β -Cyclodextrin for the Development of Deflated
1187 Spherical-Shaped Inhalable Powder. *The AAPS Journal*, 27(1), 30.
1188 <https://doi.org/10.1208/s12248-025-01015-y>

1189 Sarabandi, K., & Jafari, S. M. (2020). Effect of chitosan coating on the properties of
1190 nanoliposomes loaded with flaxseed-peptide fractions: Stability during spray-drying. *Food*
1191 *Chemistry*, 310. <https://doi.org/10.1016/j.foodchem.2019.125951>

1192 Scherließ, R., Bock, S., Bungert, N., Neustock, A., & Valentin, L. (2022). Particle engineering
1193 in dry powders for inhalation. *Eur J Pharm Sci*, 172.
1194 <https://doi.org/10.1016/j.ejps.2022.106158>

1195 Senjab, R. M., AISawafah, N., Abuwatfa, W. H., & Hussein, G. A. (2024). Advances in
1196 liposomal nanotechnology: from concept to clinics. *RSC Pharmaceuticals*, 1(5), 928–948.
1197 <https://doi.org/10.1039/D4PM00176A>

1198 Shahin, H. I., & Chablani, L. (2023). A comprehensive overview of dry powder inhalers for
1199 pulmonary drug delivery: Challenges, advances, optimization techniques, and
1200 applications. In *Journal of Drug Delivery Science and Technology* (Vol. 84). Editions de
1201 Sante. <https://doi.org/10.1016/j.jddst.2023.104553>

1202 Spahn, J. E., Zhang, F., & Smyth, H. D. C. (2022). Mixing of dry powders for inhalation: A
1203 review. In *International Journal of Pharmaceutics* (Vol. 619). Elsevier B.V.
1204 <https://doi.org/10.1016/j.ijpharm.2022.121736>

1205 Steiner, D., Schumann, L. V., & Bunjes, H. (2022). Processing of Lipid Nanodispersions into
1206 Solid Powders by Spray Drying. *Pharmaceutics*, 14(11).
1207 <https://doi.org/10.3390/pharmaceutics14112464>

1208 Susa, F., Bucca, G., Limongi, T., Cauda, V., & Pisano, R. (2021). Enhancing the preservation
1209 of liposomes: The role of cryoprotectants, lipid formulations and freezing approaches.
1210 *Cryobiology*, 98, 46–56. <https://doi.org/10.1016/j.cryobiol.2020.12.009>

1211 Tse, J. Y., Kadota, K., Imakubo, T., Uchiyama, H., & Tozuka, Y. (2021). Enhancement of the
1212 extra-fine particle fraction of levofloxacin embedded in excipient matrix formulations for
1213 dry powder inhaler using response surface methodology. *European Journal of*
1214 *Pharmaceutical Sciences*, 156. <https://doi.org/10.1016/j.ejps.2020.105600>

1215 Tunsirikongkon, A., Pyo, Y. C., Kim, D. H., Lee, S. E., & Park, J. S. (2019). Optimization of
1216 polyarginine-conjugated PEG lipid grafted proliposome formulation for enhanced cellular
1217 association of a protein drug. *Pharmaceutics*, 11(6).
1218 <https://doi.org/10.3390/pharmaceutics11060272>

1219 Usmani, O. S., & Barnes, P. J. (2012). Assessing and treating small airways disease in asthma
1220 and chronic obstructive pulmonary disease. *Annals of Medicine*, 44(2), 146–156.
1221 <https://doi.org/10.3109/07853890.2011.585656>

1222 Usmani, O. S., Scichilone, N., Mignot, B., Belmans, D., Van Holsbeke, C., De Backer, J., De
1223 Maria, R., Cuoghi, E., Topole, E., & Georges, G. (2020). Airway deposition of extrafine
1224 inhaled triple therapy in patients with copd: A model approach based on functional
1225 respiratory imaging computer simulations. *International Journal of COPD*, 15, 2433–2440.
1226 <https://doi.org/10.2147/COPD.S269001>

- 1227 Van Den Hoven, J. M., Metselaar, J. M., Storm, G., Beijnen, J. H., & Nuijen, B. (2012).
1228 Cyclodextrin as membrane protectant in spray-drying and freeze-drying of PEGylated
1229 liposomes. *International Journal of Pharmaceutics*, 438(1–2), 209–216.
1230 <https://doi.org/10.1016/j.ijpharm.2012.08.046>
- 1231 Vishali, D. A., Monisha, J., Sivakamasundari, S. K., Moses, J. A., & Anandharamakrishnan, C.
1232 (2019). Spray freeze drying: Emerging applications in drug delivery. In *Journal of*
1233 *Controlled Release* (Vol. 300, pp. 93–101). Elsevier B.V.
1234 <https://doi.org/10.1016/j.jconrel.2019.02.044>
- 1235 Wessman, P., Edwards, K., & Mahlin, D. (2010). Structural effects caused by spray- and freeze-
1236 drying of liposomes and bilayer disks. *Journal of Pharmaceutical Sciences*, 99(4), 2032–
1237 2048. <https://doi.org/10.1002/jps.21972>
- 1238 Wilhelms, B., Broscheit, J., & Shityakov, S. (2023). Chemical Analysis and Molecular Modelling
1239 of Cyclodextrin-Formulated Propofol and Its Sodium Salt to Improve Drug Solubility,
1240 Stability and Pharmacokinetics (Cytogenotoxicity). *Pharmaceutics*, 16(5).
1241 <https://doi.org/10.3390/ph16050667>
- 1242 Willis, L., Hayes, D., & Mansour, H. M. (2012). Therapeutic liposomal dry powder inhalation
1243 aerosols for targeted lung delivery. In *Lung* (Vol. 190, Number 3, pp. 251–262).
1244 <https://doi.org/10.1007/s00408-011-9360-x>
- 1245 Xu, X., Tian, F., Pan, Y., Zhang, T., Deng, L., Jiang, H., Han, J., Liu, J., Zhao, Y., & Liu, W.
1246 (2025). Emerging mechanistic insights into liposomal stability: Full process management
1247 from production and storage to food application. In *Chemical Engineering Journal* (Vol.
1248 505). Elsevier B.V. <https://doi.org/10.1016/j.cej.2025.159552>
- 1249 Yan, X., & Sha, X. (2023). Nanoparticle-Mediated Strategies for Enhanced Drug Penetration
1250 and Retention in the Airway Mucosa. In *Pharmaceutics* (Vol. 15, Number 10).
1251 Multidisciplinary Digital Publishing Institute (MDPI).
1252 <https://doi.org/10.3390/pharmaceutics15102457>
- 1253 Yergey, A. L., Blank, P. S., Cologna, S. M., Backlund, P. S., Porter, F. D., & Darling, A. J. (2017).
1254 Characterization of hydroxypropyl-beta-cyclodextrins used in the treatment of Niemann-
1255 Pick Disease type C1. *PLoS ONE*, 12(4). <https://doi.org/10.1371/journal.pone.0175478>
- 1256 Yu, J. Y., Chuesiang, P., Shin, G. H., & Park, H. J. (2021). Post-processing techniques for the
1257 improvement of liposome stability. *Pharmaceutics*, 13(7).
1258 <https://doi.org/10.3390/pharmaceutics13071023>
- 1259 Zhang, J., Huang, Y., Shen, W., Zeng, Y., Miao, Y., Feng, N., & Ci, T. (2025). Effects of Surface
1260 Charge of Inhaled Liposomes on Drug Efficacy and Biocompatibility. *Pharmaceutics*,
1261 17(3). <https://doi.org/10.3390/pharmaceutics17030329>
- 1262 Zhao, J., Qin, L., Song, R., Su, J., Yuan, Y., Zhang, X., & Mao, S. (2022). Elucidating inhaled
1263 liposome surface charge on its interaction with biological barriers in the lung. *European*
1264 *Journal of Pharmaceutics and Biopharmaceutics*, 172, 101–111.
1265 <https://doi.org/10.1016/j.ejpb.2022.01.009>
- 1266 Zheng, Y., & Chow, A. H. L. (2009). Production and characterization of a spray-dried
1267 hydroxypropyl- β - cyclodextrin/ quercetin complex Spray-dried hydroxypropyl- β -
1268 cyclodextrin/ quercetin complex. *Drug Development and Industrial Pharmacy*, 35(6), 727–
1269 734. <https://doi.org/10.1080/03639040802526805>

1270 Ziaee, A., Albadarin, A. B., Padrela, L., Femmer, T., O'Reilly, E., & Walker, G. (2019). Spray
1271 drying of pharmaceuticals and biopharmaceuticals: Critical parameters and experimental
1272 process optimization approaches. In *Eur J Pharm Sci* (Vol. 127, pp. 300–318). Elsevier
1273 B.V. <https://doi.org/10.1016/j.ejps.2018.10.026>

1274 Zillen, D., Beugeling, M., Hinrichs, W. L. J., Frijlink, H. W., & Grasmeijer, F. (2021). Natural and
1275 bioinspired excipients for dry powder inhalation formulations. In *Current Opinion in Colloid
1276 and Interface Science* (Vol. 56). Elsevier Ltd. <https://doi.org/10.1016/j.cocis.2021.101497>

1277 Zimmermann, C. M., Baldassi, D., Chan, K., Adams, N. B. P., Neumann, A., Porras-Gonzalez,
1278 D. L., Wei, X., Kneidinger, N., Stoleriu, M. G., Burgstaller, G., Witzigmann, D., Luciani, P.,
1279 & Merkel, O. M. (2022). Spray drying siRNA-lipid nanoparticles for dry powder pulmonary
1280 delivery. *Journal of Controlled Release*, 351, 137–150.
1281 <https://doi.org/10.1016/j.jconrel.2022.09.021>

1282

1283

1284

1285

1286

1287

1288

1289

1290

1291

1292

1293

1294

1295

1296

1297

1298

1299

1300

1301

1302 SUPPLEMENTARY DATA

1303 **Supplementary Data A:** Summary of DOE_A tested parameters and corresponding responses.

1304

Tested SD parameters and carbohydrate matrix

Responses

Random Block	Excipient	Inlet temperature (°C)	Flowrate (rpm)	Nozzle Gas Pressure (bar)	Cyclone gas pressure (bar)	Particle size (µm)	SD yield (%)	Water content (%)	Sf/Si size ratio	PdI upon SD
1	trehalose	120	25	1	0.05	3.099	72.915	2.229	0.946	0.393
1	HPβCD	120	25	1	0.3	3.962	75.707	2.293	0.923	0.291
2	trehalose	90	88	2.5	0.18	2.127	72.873	4.806	1.045	0.631
2	trehalose	60	150	1	0.05	4.26	63.769	5.422	0.995	0.465
3	trehalose	120	25	4	0.3	1.389	63.798	3.435	1.207	0.532
3	HPβCD	60	25	4	0.3	1.644	75.807	5.308	0.938	0.373
4	HPβCD	120	150	1	0.05	4.699	75.808	4.339	0.87	0.402
4	trehalose	90	88	2.5	0.18	2.341	72.912	3.874	0.998	0.471
5	trehalose	90	150	1	0.3	5.07	72.922	5.594	0.817	0.409
5	HPβCD	60	25	1	0.18	3.378	85.199	6.264	0.691	0.39
6	trehalose	120	150	2.5	0.3	2.63	81.996	3.654	0.891	0.472
6	HPβCD	120	150	4	0.3	2.055	66.273	5.719	0.75	0.261
7	HPβCD	60	88	1	0.05	3.134	75.657	8.813	0.759	0.332
7	trehalose	120	150	4	0.05	1.847	72.972	5.447	0.966	0.395
8	trehalose	60	150	4	0.3	/	9.119	9.111	0.958	0.358
8	HPβCD	90	88	2.5	0.18	2.235	75.657	6.759	0.904	0.327
9	trehalose	60	25	4	0.05	1.68	72.94	5.323	0.85	0.428
9	HPβCD	60	150	4	0.05	1.596	75.731	6.733	0.921	0.428
10	trehalose	120	88	1	0.3	4.721	72.814	4.151	0.968	0.441
10	HPβCD	90	25	1	0.05	3.787	75.741	5.072	1.111	0.454
11	HPβCD	120	25	4	0.05	1.715	66.264	5.04	1.104	0.477
11	trehalose	60	25	1	0.3	3.456	59.226	4.8	0.996	0.464
12	trehalose	120	150	1	0.18	5.416	72.982	4.066	0.889	0.474
12	HPβCD	60	150	1	0.3	5.301	56.786	5.484	0.918	0.401

1305

1306 **Supplementary Data B:** Summary of drying parameters showing significant effects on
1307 response variables (DPI properties and liposomes integrity) identified through statistical
1308 analysis in DOE_A.

	Response variable	Significant drying parameters
<i>DPI properties</i>	Particle size	<ul style="list-style-type: none"> • Cyclone gas pressure (p < 0.0001) • Excipient*Cyclone gas pressure (p < 0.05) • Excipient*Flowrate (p < 0.0001) • Excipient*Inlet temperature (p < 0.0001) • Flowrate (p < 0.0001) • Flowrate*Nozzle gas pressure (p < 0.0001) • Inlet temperature (p < 0.0001) • Inlet temperature*Cyclone gas pressure (p < 0.05) • Nozzle gas pressure (p < 0.0001)
	Drying Yield	<ul style="list-style-type: none"> • Excipient (p < 0.05) • Cyclone gas pressure (p < 0.05) • Excipient*Flowrate (p < 0.05)

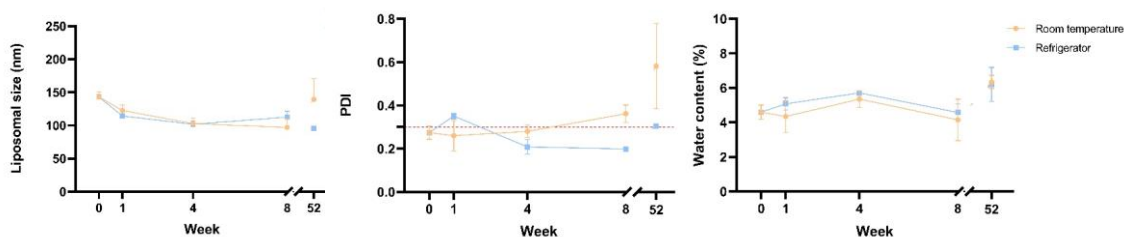
Liposomes integrity

Moisture content
Size ratio (Sf/Si)
Pdl

- Inlet temperature*Nozzle Gas pressure ($p < 0.05$)
- Nozzle gas pressure*Nozzle gas pressure ($p < 0.05$)
- Inlet temperature ($p < 0.05$)
- Inlet temperature*Flowrate ($p < 0.05$)

1309

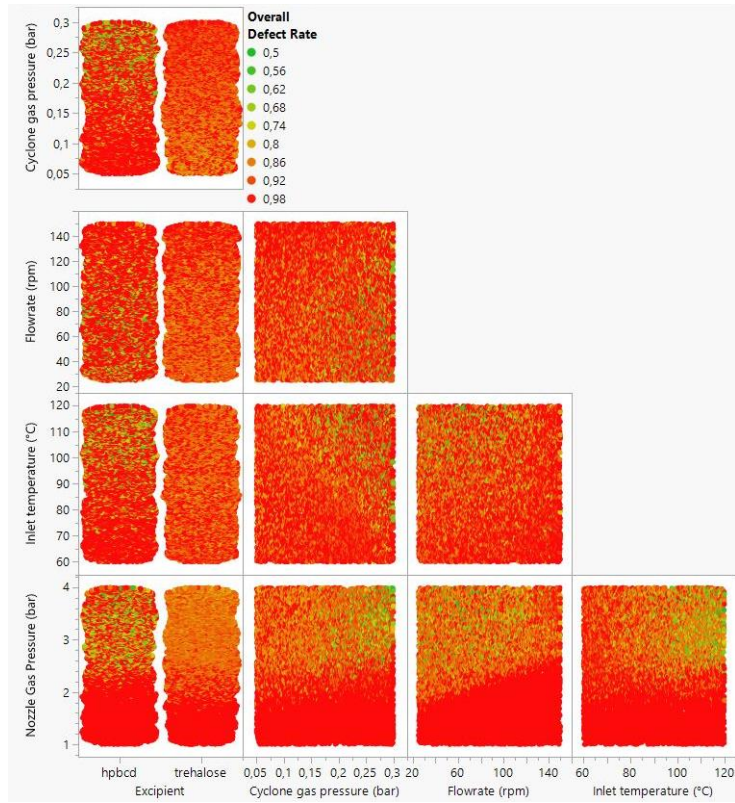
1310 **Supplementary Data C: Long-term stability of DOE_A processed empty liposomal powders**



1311 Long-term stability was evaluated for empty liposomal powders produced by DOE_A under
1312 optimal processing conditions using HP β CD, as trehalose-based formulations were not
1313 retained after drying. Liposomal powders were stored at 5 °C and at room temperature, and
1314 physicochemical properties were monitored over a 12-month period.

1315 Throughout the storage period, liposomal integrity was largely preserved under both
1316 conditions, as evidenced by stable mean particle size values. A slight reduction in mean
1317 liposomal diameter (from approximately 140 to 120 nm) was observed over time but remained
1318 within the expected variability of DLS measurements and did not indicate structural
1319 destabilization. Pdl values remained stable during refrigerated storage, whereas a gradual
1320 increase in Pdl was detected at room temperature, suggesting the onset of increased size
1321 heterogeneity. In parallel, powder water content remained stable at approximately 5%
1322 throughout the study, which is within acceptable limits for inhalable dried formulations.

1323 While this short-term stability assessment is encouraging, further studies conducted under
1324 ICH-recommended conditions and using final packaging configurations will be required to
1325 confirm long-term stability and ensure reproducibility in clinically relevant delivery
1326 systems. **Supplementary Data D: DOE_A's design space.** The design space analysis revealed
1327 that only a narrow range of spray-drying parameters and carbohydrate matrix compositions
1328 achieved the desired conditions (DPI parameters suitable for inhalation, while preserving
1329 liposome integrity), as shown by the green dots, highlighting the complexity and critical
1330 importance of this experimental design.



1331

1332

1333 **Supplementary Data E: Summary of DOE_B tested parameters and corresponding responses.**

Whole Plots	Tested parameters				Responses			
	API nature	DSPE-PEG2000 content (%)	L/C ratio (%)	Water content (%)	Particle size (µm)	Release upon SD (%)	Sf/Si ratio	PdI
1	SAL	10	5.5	3.79	2.66	85.31	0.94	0.219
1	SAL	10	1	1.82	2.59	100	0.94	0.251
1	SAL	10	10	3	2.48	70.27	0.91	0.215
2	SAL	6.25	1	4.06	2.72	100	0.91	0.257
2	SAL	6.25	5.5	3.32	2.57	81.63	0.88	0.216
2	SAL	6.25	10	1.96	2.58	67.7	0.87	0.214
3	SAL	2.5	10	3.4	2.69	71.36	0.89	0.216
3	SAL	2.5	5.5	2.7	2.7	95.01	0.98	0.231
3	SAL	2.5	1	1.74	2.48	100	1.04	0.269
4	BUD	10	5.5	6.22	2.44	39.6	0.93	0.205
4	BUD	10	10	4.16	2.52	37.5	0.94	0.186
4	BUD	10	1	4.29	2.71	46.29	0.93	0.215
5	BUD	6.25	10	5.43	2.537	22.59	0.91	0.192

5	BUD	6.25	5.5	5.2	3.567	35.08	0.96	0.227
6	BUD	2.5	1	3.49	4.489	31.42	0.97	0.238
6	BUD	2.5	10	3	2.74	20.18	0.9	0.235
7	BUD	6.25	1	4.68	2.549	36.58	0.94	0.208
7	BUD	6.25	5.5	2.18	2.463	27.37	0.93	0.213

1334

1335

1336 **Supplementary Data F:** Summary of tested parameters (API nature, L/C ratio and PEGylated
1337 lipid content) showing significant effects on response variables (liposomes integrity) identified
1338 through statistical analysis in DOE_B.

1339

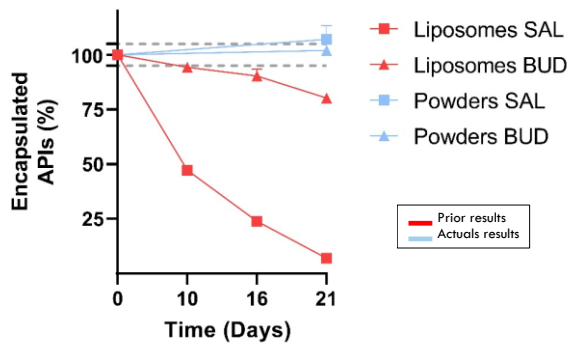
	<i>Response variable</i>	<i>Significant drying parameters</i>
<i>Liposomes integrity</i>	API release	<ul style="list-style-type: none"> • API nature (p < 0.05) • L/C ratio (p < 0.0001)
	Size ratio (Sf/Si)	<ul style="list-style-type: none"> • API nature (p < 0.05) • L/C ratio (p < 0.05)
	Pdl	<ul style="list-style-type: none"> • Lipid content (p < 0.05)

1340

1341

1342 **Supplementary Data G:** Short-term stability comparison of liquid and spray-dried liposomal
1343 formulations

1344 An initial stability study was conducted comparing the stability of the liposome suspension
1345 obtained after the PGSS process with that of the dried liposomes under BUD-optimized
1346 condition. Both the powders and the liposome suspensions were stored at +4 °C. This study
1347 was inspired by and supplemented with previously published results from Penoy *et al.* on the
1348 same liposome composition and production (Penoy et al., 2022). When examining the results,
1349 Figure below shows that, for non-dried liposomes, after three weeks, the release reached 93 ± 0.20
1350 ± 0.20 for SAL and $19.74 \pm 1.77\%$ for BUD. In contrast, in the spray-dried powders,
1351 encapsulation remained stable between time zero and three weeks. In addition to its drying
1352 protective effect, HP β CD also serves as an effective stabilizing agent after drying. Unlike other
1353 carbohydrates matrix such as trehalose or sucrose, HP β CD possesses a high Tg above 200
1354 °C and exhibits low hygroscopicity, and exhibits low hygroscopicity, which helps preserve the
1355 amorphous glassy state during storage. This unique combination of properties ensures
1356 superior long-term stability of dried liposomal formulations (Chang et al., 2020; Haeuser et al.,
1357 2019; Hammoud et al., 2019; Milani et al., 2020).



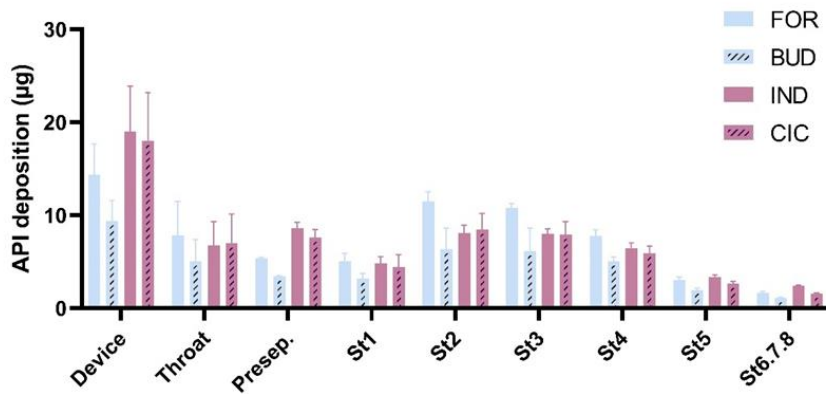
1358

1359 *Figure: Stability of liposomal formulations over time, showing the percentage of encapsulated API for PGSS-processed*
 1360 *suspensions versus spray-dried powders under BUD-optimized conditions. Values are normalized to 100% at time*
 1361 *zero. Analyses were performed in triplicates (n = 3) and results are presented as mean ± standard deviation.*

1362

1363 **Supplementary Data H: Stage-by-stage NGI deposition profiles of the different APIs at 100**
 1364 **L/min.**

1365



1366